Article

Immunity

Cross-Regulation of Two Type I Interferon Signaling Pathways in Plasmacytoid Dendritic Cells Controls Anti-malaria Immunity and Host Mortality

Graphical Abstract

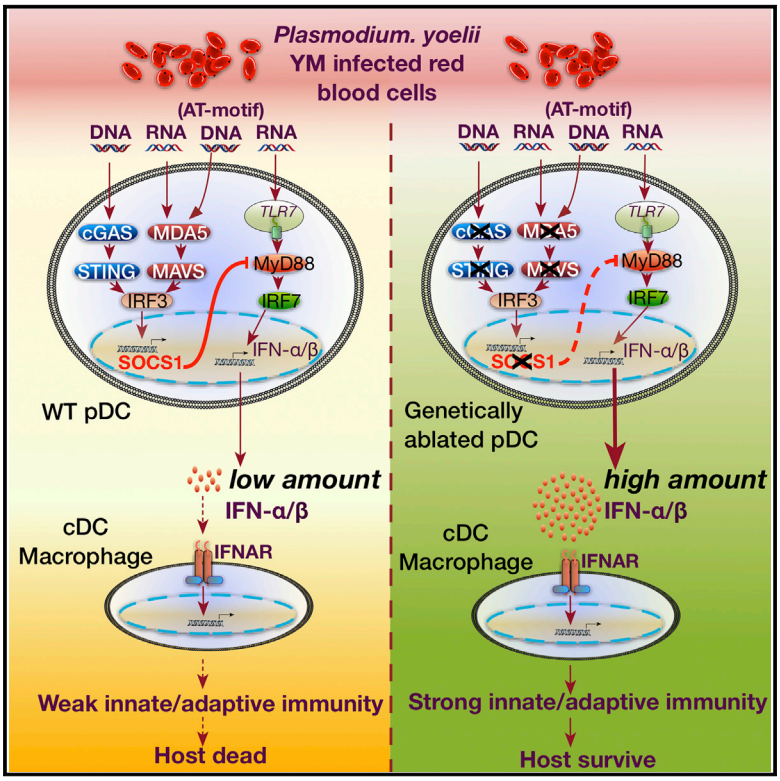

Highlights

- cGAS functions as a DNA sensor in vivo for detecting malaria genomic DNA
- STING- and MAVS-mediated signaling induces a negative regulator SOCS1 expression
- SOCS1 inhibits MyD88-mediated type I IFN signaling in pDCs
- Type I IFN produced by pDCs activates cDCs and macrophages for adaptive immunity

Authors

Xiao Yu, Baowei Cai, Mingjun Wang, ..., Helen Y. Wang, Xin-zhuan Su, Rong-Fu Wang

Correspondence

xsu@niaid.nih.gov (X.-z.S.), rwang3@houstonmethodist.org (R.-F.W.)

In Brief

Malaria is a worldwide deadly infectious disease; how type I IFN signaling is regulated in response to malaria infection remains poorly understood. Yu et al. identify a cross-regulatory mechanism of two type I IFN signaling pathways in plasmacytoid DCs, which is critical for generating protective immunity against lethal malaria infection.

Yu et al., 2016, Immunity *45*, 1093–1107
November 15, 2016
http://dx.doi.org/10.1016/j.immuni.2016.10.001

Immunity
Article

Cross-Regulation of Two Type I Interferon Signaling Pathways in Plasmacytoid Dendritic Cells Controls Anti-malaria Immunity and Host Mortality

Xiao Yu,[1,3,8] Baowei Cai,[3,4,8] Mingjun Wang,[2,3] Peng Tan,[3,7] Xilai Ding,[3] Jian Wu,[5] Jian Li,[4] Qingtian Li,[3] Pinghua Liu,[3] Changsheng Xing,[3] Helen Y. Wang,[3] Xin-zhuan Su,[4,5,*] and Rong-Fu Wang[3,6,7,9,*]
[1]School of Life Sciences
[2]Zhongshan School of Medicine
Sun Yat-Sen University, 510275 Guangzhou, P.R. China
[3]Center for Inflammation and Epigenetics, Houston Methodist Research Institute, Houston, TX 77030, USA
[4]State Key Laboratory of Cellular Stress Biology, Innovation Center for Cell Biology, School of Life Sciences, Xiamen University, Xiamen, 361005 Fujian, P.R. China
[5]Laboratory of Malaria and Vector Research, National Institute of Allergy and Infectious Diseases, National Institutes of Health, Bethesda, MD 20892, USA
[6]Department of Microbiology and Immunology, Weill Cornell Medicine, Cornell University, New York, NY 10065, USA
[7]Institute of Biosciences and Technology, College of Medicine, Texas A&M University, Houston, TX 77030, USA
[8]Co-first author
[9]Lead Contact
*Correspondence: xsu@niaid.nih.gov (X.-z.S.), rwang3@houstonmethodist.org (R.-F.W.)
http://dx.doi.org/10.1016/j.immuni.2016.10.001

SUMMARY

Type I interferon (IFN) is critical for controlling pathogen infection; however, its regulatory mechanisms in plasmacytoid cells (pDCs) still remain unclear. Here, we have shown that nucleic acid sensors cGAS-, STING-, MDA5-, MAVS-, or transcription factor IRF3-deficient mice produced high amounts of type I IFN-α and IFN-β (IFN-α/β) in the serum and were resistant to lethal *plasmodium yoelii* YM infection. Robust IFN-α/β production was abolished when gene encoding nucleic acid sensor TLR7, signaling adaptor MyD88, or transcription factor IRF7 was ablated or pDCs were depleted. Further, we identified SOCS1 as a key negative regulator to inhibit MyD88-dependent type I IFN signaling in pDCs. Finally, we have demonstrated that pDCs, cDCs, and macrophages were required for generating IFN-α/β-induced subsequent protective immunity. Thus, our findings have identified a critical regulatory mechanism of type I IFN signaling in pDCs and stage-specific function of immune cells in generating potent immunity against lethal YM infection.

INTRODUCTION

Type I interferon (IFN) and NF-κB pathways play key roles in controlling disease pathogenesis (Goubau et al., 2013; Paludan and Bowie, 2013; Takeuchi and Akira, 2010). The innate immune response serves as the first line of defense against invading pathogens and relies on the recognition of pathogen-associated molecular patterns (PAMPs) by several classes of pattern-recognition receptors (PRRs), including Toll-like receptors (TLRs), nucleotide-binding domain and leucine-rich repeat containing gene family (NLRs), and RIG-I-like receptors (RLRs) (Goubau et al., 2013; Paludan and Bowie, 2013; Takeuchi and Akira, 2010). Activation of most TLRs leads to the recruitment of a common adaptor molecule, MyD88, which acts on a series of downstream signaling molecules to trigger the NF-κB pathway (Goubau et al., 2013; Hayden and Ghosh, 2008; Paludan and Bowie, 2013), whereas stimulation of TLR7 and TLR9 in specialized plasmacytoid dendritic cells (pDCs) can trigger robust MyD88-dependent IFN regulatory factor (IRF) 7 transcription factor-mediated type I IFN signaling and produce large amounts of IFN-α and IFN-β (IFN-α/β) in response to viral infection (Liu, 2005; Wang et al., 2011). By contrast, activation of cytosolic RNA sensors (RIG-I and MDA5) recruits the mitochondrial antiviral-signaling protein (MAVS) adaptor protein, while stimulation of DNA sensors recruits stimulator of IFN genes (STING), which both result in triggering IRF3-mediated type I IFN signaling (Goubau et al., 2013; Paludan and Bowie, 2013; Sun et al., 2013; Takeuchi and Akira, 2010). Innate immune responses must be tightly regulated to maintain immune balance, but how these signaling pathways are regulated in vivo, particularly in response to malaria infection, remains unresolved.

Malaria is a deadly infectious disease and is responsible for up to 0.5 million deaths each year (Miller et al., 2013). Lack of effective vaccines against malaria has been one of the major limiting factors in controlling the disease (Riley and Stewart, 2013). The incomplete understanding of the malaria-strain-specific response and regulatory mechanisms impedes our ability to develop effective malaria vaccines (Langhorne et al., 2008; Riley and Stewart, 2013; Stevenson and Riley, 2004). Recent studies show that the liver stage of infection can induce type I IFN signaling activation, either through the cytosolic PRRs, MDA5-MAVS pathway (Liehl et al., 2014), or multiple mechanisms (Miller

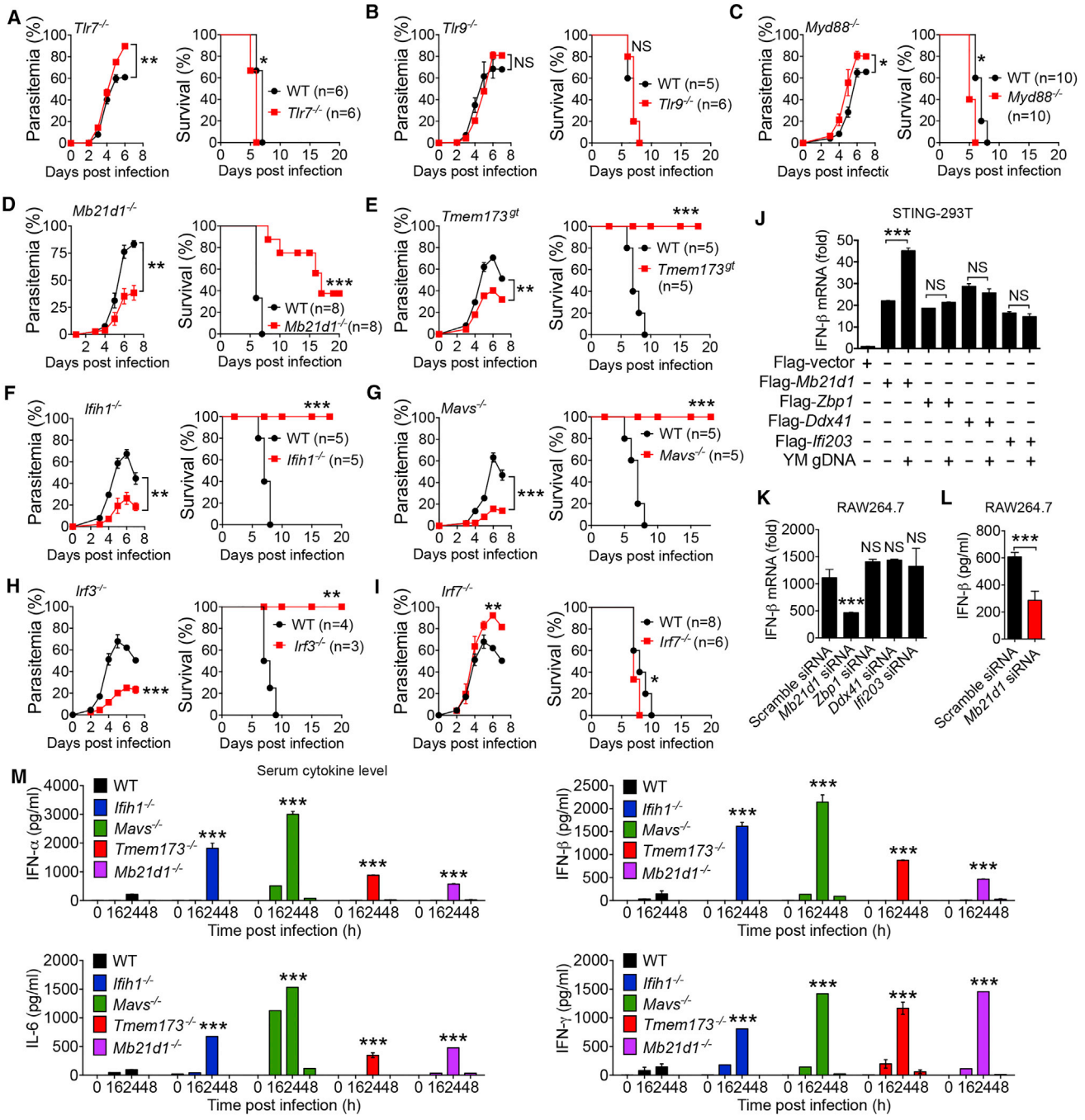

Figure 1. Mice Deficient in cGAS, STING, MDA5, MAVS, or IRF3, but Not in TLR Signaling Molecules, Are Protected from YM Infection

(A–C) Daily parasitemias and mortality rates of WT (black lines) and TLR-deficient mice (red lines) after YM (0.5×10^6 iRBCs) infection: *Tlr7*$^{-/-}$ (A), *Tlr9*$^{-/-}$ (B), and *Myd88*$^{-/-}$ (C).

(D–I) Daily parasitemias and mortality rates of WT (black lines) and indicated deficient mice (red lines) after YM infection: *Mb21d1*$^{-/-}$ (D), *Tmem173*^{gt} (E), *Ifih1*$^{-/-}$ (F), *Mavs*$^{-/-}$ (G), *Irf3*$^{-/-}$ (H), and *Irf7*$^{-/-}$ (I) mice.

(J) Quantitative analysis of IFN-β mRNA in STING stably expressing 293T cells transfected with Flag-*Mb21d1*, *Zbp1*, *Ddx41*, or *Ifi203* followed by YM gDNA stimulation for 18 hr.

(K) Quantitative analysis of IFN-β mRNA in RAW264.7 cells transfected with *Mb21d1*-, *Zbp1*-, *Ddx41*-, *Ifi203*-specific siRNA, or scramble siRNA for 48 hr, followed by YM gDNA stimulation for 6 hr.

(L) RAW264.7 cells were transfected with *Mb21d1*-specific siRNA or scramble siRNA, followed by YM gDNA stimulation for 24 hr. Cell supernatants were collected for ELISA analysis.

(legend continued on next page)

et al., 2014). After the liver stage of infection and expansion, merozoites are released into the blood and infect red blood cells (iRBCs), which activate several key signaling pathways, including NF-κB, type I IFN, and the inflammasome (Gazzinelli et al., 2014; Miller et al., 2014; Riley and Stewart, 2013; Wu et al., 2014). However, the role of TLRs and type I IFN in malaria blood-stage infection is unclear or remain controversial (Baccarella et al., 2013; Gowda et al., 2012; Haque et al., 2014; Liehl and Mota, 2012; Sharma et al., 2011; Togbe et al., 2007; Wu et al., 2010). Therefore, we have used a lethal malaria *plasmodium yoelii* YM (YM for short) strain as a model to probe the molecular signaling pathways and mechanisms of host immune response during blood stage infection.

In this study, we identified cGAS as a key DNA sensor that triggers the type I IFN signaling pathway after YM infection. cGAS-, STING-, MAVS-, or MDA5-deficient mice were resistant to lethal YM infection compared with wild-type (WT) mice. High serum amounts of IFN-α/β in these genetically deficient mice were abolished upon depletion of pDC or ablation of *Tlr7*, *Myd88*, and *Irf7*. Our experiments further revealed that the STING- and MAVS-mediated type I IFN pathway induced SOCS1 expression, which potently inhibited MyD88-dependent type I IFN signaling in pDCs. Furthermore, we showed that early robust IFN-α/β production by pDCs in genetically ablated mice during the first 24 hr of YM infection subsequently activated cDCs and macrophages, which, in turn, induced T- and B-cell-mediated adaptive immune responses against malaria infection.

RESULTS

Mice Deficient in cGAS, STING, MDA5, MAVS, or IRF3 Are Resistant to YM Infection

Since the role of TLRs in defending against different malaria species remains controversial (Baccarella et al., 2013; Gowda et al., 2012; Togbe et al., 2007), we first investigated whether TLRs and their downstream signaling molecules play a role in controlling lethal YM infection. We infected *Tlr2*$^{-/-}$, *Tlr3*$^{-/-}$, *Tlr4*$^{-/-}$, *Tlr7*$^{-/-}$, *Tlr9*$^{-/-}$, *Ticam1*$^{-/-}$ (coding for TRIF), *Myd88*$^{-/-}$, and WT mice by intraperitoneal (i.p.) injection of YM-iRBCs. We found that WT and genetically deleted mice died within 8 days after infection (Figures 1A–1C and S1A–S1D). Notably, *Tlr7*$^{-/-}$ and *Myd88*$^{-/-}$ mice showed increased parasitemia and died sooner after infection than WT mice, suggesting that TLR7 and MyD88 may play a role in the control of parasitemia and host mortality.

To test whether RNA and DNA sensor-mediated type I IFN signaling plays a role in host immune responses to YM infection, we infected *Mb21d1*$^{-/-}$ (coding for cGAS), *Tmem173*^{gt} (coding for STING), *Ifih1*$^{-/-}$ (coding for MDA5), and *Mavs*$^{-/-}$ mice with YM. We found that these genetically ablated mice remarkably reduced parasitemia compared with WT mice. *Tmem173*^{gt}, *Ifih1*$^{-/-}$, and *Mavs*$^{-/-}$ mice were completely resistant to YM infection, whereas *Mb21d1*$^{-/-}$ mice showed partial protection (Figures 1D–1G). Furthermore, YM infection was completely cleared in *Ifih1*$^{-/-}$, *Mavs*$^{-/-}$, and *Tmem173*^{gt} mice within 4 weeks (Figure S1F). However, mice with ablation of the *Ddx58* gene (coding for RIG-I) showed no difference in malaria parasitemia and host death, compared with WT mice (Figure S1E). IRF3 is a key factor for stimulating type I IFN signaling for IFN-β production in almost all cell types, whereas IRF7 is responsible for activating type I IFN signaling to produce IFN-α/β only in pDCs (Liu, 2005; Wang et al., 2011). Infection of *Irf3*$^{-/-}$ and *Irf7*$^{-/-}$ mice with YM revealed that *Irf3*$^{-/-}$ mice, but not *Irf7*$^{-/-}$ mice, remarkably reduced parasitemia and were resistant to YM infection (Figures 1H and 1I). Collectively, these results suggest that activation of cGAS-STING and MDA5-MAVS-mediated IRF3-dependent type I IFN signaling leads to a lethal phenotype of YM infection.

Identification of cGAS as a Malaria DNA Sensor and Robust Production of IFN-α/β in cGAS-, STING-, MDA5-, or MAVS-Deficient Mice

To understand how cGAS-, STING-, MDA5-, and MAVS-deficient mice were resistant to YM infection, we first determined whether cGAS and MDA5 functioned as DNA or RNA sensors for detecting YM genomic DNAs (gDNAs) or RNAs. We found that both purified YM gDNA and RNA could induce IFN-β mRNA expression in RAW264.7 cells (Figure S1G), which is in agreement with other studies showing that malaria RNA can be detected by a MDA5 sensor (Liehl et al., 2014; Wu et al., 2014). As expected, in vitro stimulation with YM gDNA or RNA showed impaired or completely abolished activation of IFN-β mRNA and protein in bone-marrow-derived conventional DCs (cDCs) from MDA5-, MAVS-, and STING-deficient mice compared to cDCs from WT mice (Figure S1H). Although STING has been shown to play an important role in the host response to AT-rich malarial DNA (Sharma et al., 2011), it is not clear which DNA sensors are responsible for recognizing YM gDNA and activating STING-mediated type I IFN signaling. To this end, we transfected 293T-STING stable cells with plasmids containing the gene encoding one of four putative DNA sensors (cGAS, DAI, DDX41, or IFI16) followed by YM gDNA stimulation. Ectopic expression of *Mb21d1*, but not *Zbp1*, *Ddx41*, or *Ifi203*, induced IFN-β mRNA expression after YM gDNA treatment (Figure 1J). Consistently, silencing of *Mb21d1*, but not *Zbp1*, *Ddx41*, or *Ifi203*, by specific siRNAs in RAW264.7 cells markedly reduced IFN-β mRNA and protein after YM gDNA treatment (Figures 1K, 1L, and S1I), suggesting that cGAS functions as a DNA sensor for detecting YM gDNA and inducing STING-mediated type I IFN signaling.

Previous studies showed that type I IFN signaling inhibits type II IFN (IFN-γ) or adaptive immune responses upon malaria and viral infection (Haque et al., 2011; Palomo et al., 2013; Teijaro et al., 2013; Teles et al., 2013; Wilson et al., 2013). To this end, we examined the serum amounts of IFN-α/β, IL-6, and IFN-γ in WT mice during YM infection and found that these cytokines were increased and peaked at 24 hr post infection and then completely disappeared in WT mice (Figure S1J). However, the serum amounts of IFN-α/β, IL-6, and IFN-γ in MDA5-, MAVS-, STING-, and cGAS-deficient mice were much higher than in

(M) WT and indicated deficient mice were infected with YM. Serum amounts of IFN-α/β, IL-6, and IFN-γ were determined by ELISA.
Data are representative of three independent experiments and are plotted as the mean ± SD. *$p < 0.05$, **$p < 0.01$, ***$p < 0.001$ versus corresponding control. NS, not significant.
See also Figure S1.

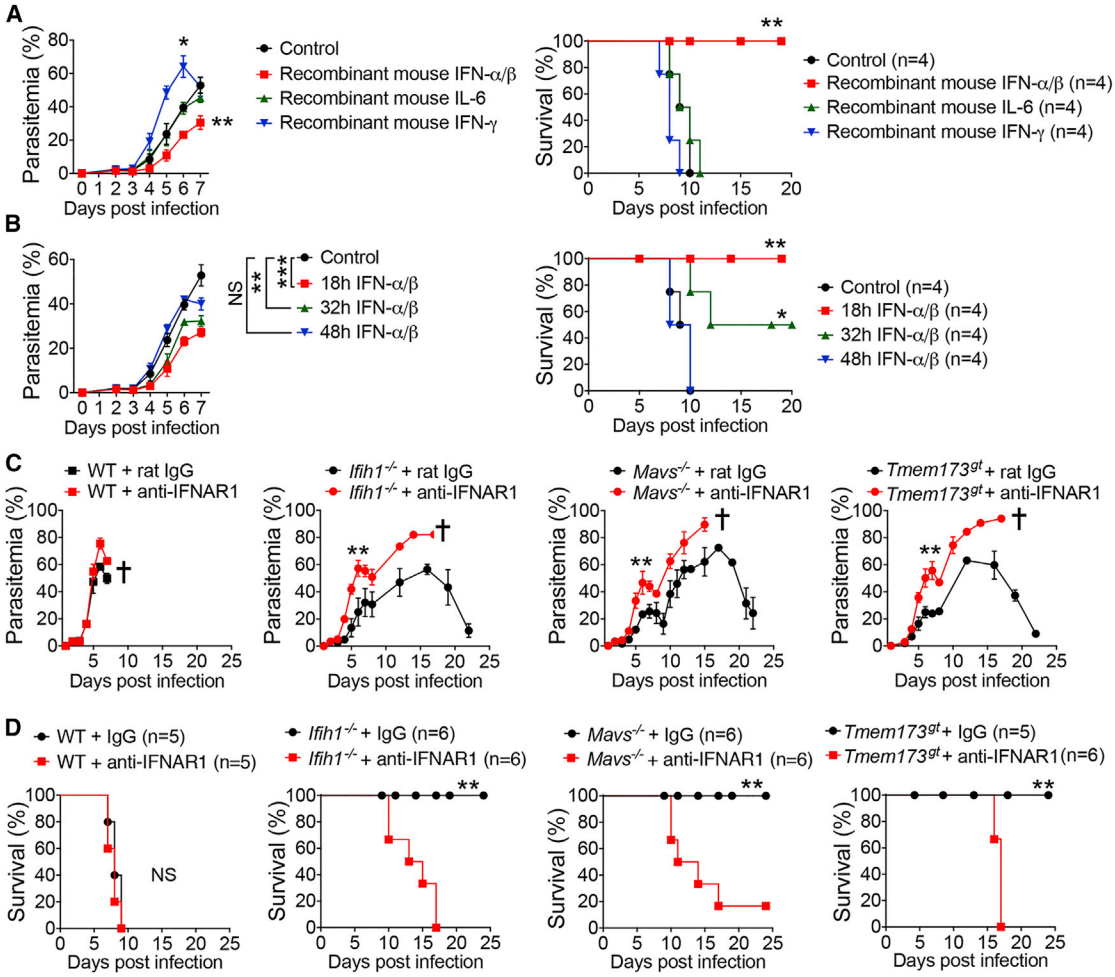

Figure 2. Type I IFN and Blockade of IFNAR Determine the Fate of YM-Infected Mice

(A) Parasitemias and mortality rates of WT mice infected with YM, followed by i.v. administration of recombinant mouse IFN-α/β, IL-6, IFN-γ, or control BSA protein at 18 hr post infection.

(B) Parasitemias and mortality rates of WT mice infected with YM, followed by i.v. administration of recombinant mouse IFN-α/β at 18, 32, or 48 hr post infection.

(C and D) Parasitemias (C) and mortality rates (D) of WT, *Ifih1*$^{-/-}$, *Mavs*$^{-/-}$, and *Tmem173*^{gt} mice treated with anti-IFNAR1 blocking antibody at days −1, 2, 4, and 6 (500 μg), followed by infection with YM (2×10^6 iRBCs).

Data are representative of three independent experiments and are plotted as the mean ± SD. *$p < 0.05$, **$p < 0.01$, ***$p < 0.001$ versus corresponding control. NS, not significant. † denotes mouse death.

See also Figure S2.

WT mice at 24 hr after YM infection (Figure 1M), suggesting that MDA5, MAVS, STING, or cGAS deficiency enhances type I IFN production in vivo after YM infection.

Robust Production of IFN-α/β Is Required for Generating Immunity against YM Infection

To determine which cytokines are responsible for generating protective immunity against YM infection, we injected WT mice with exogenous recombinant IFN-α/β, IFN-γ, or IL-6 and then tested their ability to inhibit parasitemia and reduce host mortality after YM infection. WT mice treated with IFN-α/β after YM infection had markedly decreased parasitemia and host mortality, but treatment with IL-6 or IFN-γ failed to do so (Figure 2A). Since the production of IFN-α/β in serum peaked at 24 hr after YM infection and then disappeared, we asked whether the timing of cytokine treatment was important for protective immunity. We performed similar experiments with cytokine injections at different time points and found that the amounts of IFN-α/β-mediated protection were the highest at 18 hr after YM infection, intermediate at 32 hr, and the lowest at 48 hr (Figure 2B). These results suggest that timing of IFN-α/β administration or in vivo production is critical for inducing protective immunity against YM infection.

Next, we sought to determine the molecular mechanisms of how an early robust burst of IFN-α/β can generate potent protective immune responses. We hypothesized that IFN-α/β may initiate a cascade of signaling events to generate potent immune responses. As the first step, we asked whether IFN-α/β-mediated activation of IFNAR (IFN-α/β receptor) is required for controlling parasitemia and host mortality. We blocked type I IFN

signaling in *Ifih1*$^{-/-}$, *Mavs*$^{-/-}$, and *Tmem173*^{gt} mice by administering anti-IFNAR1 antibody. Although anti-IFNAR1 treatment did not have much effect on the production of IFN-α/β, IFN-γ, and IL-6 in *Mavs*$^{-/-}$ mice (Figure S2A), the *Ifih1*$^{-/-}$, *Mavs*$^{-/-}$, and *Tmem173*^{gt} mice treated with anti-IFNAR1 antibody with a single injection at 1 day before infection (i.e., day −1) or four injections at days −1, 2, 4, and 6 showed increased parasitemias and died around day 15 (Figures 2C, 2D, and S2B), suggesting that the IFN-α/β-mediated downstream signaling pathway is critical in controlling parasitemia and host mortality. To further test whether IFN-α/β-induced immunity requires IFNAR and its downstream signaling, we infected *Ifnar1*$^{-/-}$ mice with YM and found comparable low amounts of IFN-α/β, IL-6, and IFN-γ in serum compared with those in WT mice (Figure S2C). Whereas WT mice treated with exogenous recombinant IFN-α/β became resistant to YM infection, *Ifnar1*$^{-/-}$ mice with recombinant IFN-α/β did not reduce parasitemia and mortality (Figure S2D), indicating that IFNAR is required for IFN-α/β-mediated protective immunity against YM infection.

Role of TLR7-MyD88-IRF7 Type I IFN Signaling in Robust Production of IFN-α/β

Next, we sought to identify the key signaling pathways that are responsible for the robust production of IFN-α/β in *Ifih1*$^{-/-}$, *Mavs*$^{-/-}$, and *Tmem173*^{gt} mice at 24 hr after YM infection. We first asked whether ablation of the *Tlr7*, *Myd88*, or *Irf7* gene could reduce IFN-α/β production and reverse the resistant phenotypes of *Ifih1*$^{-/-}$, *Mavs*$^{-/-}$, and *Tmem173*^{gt} mice to YM infection. To test this possibility, we generated *Ifih1*$^{-/-}$:*Myd88*$^{-/-}$, *Mavs*$^{-/-}$:*Myd88*$^{-/-}$, and *Tmem173*^{gt}:*Myd88*$^{-/-}$ mice and then infected them, along with WT, *Ifih1*$^{-/-}$, *Mavs*$^{-/-}$, and *Tmem173*^{gt} mice, with YM. As expected, serum amounts of IFN-α/β were very high in *Ifih1*$^{-/-}$, *Mavs*$^{-/-}$, and *Tmem173*^{gt} mice. However, we could not detect any IFN-α/β in the sera of *Ifih1*$^{-/-}$:*Myd88*$^{-/-}$, *Mavs*$^{-/-}$:*Myd88*$^{-/-}$, and *Tmem173*^{gt}:*Myd88*$^{-/-}$ mice or in the sera of *Myd88*$^{-/-}$ mice (Figures 3A, S3A, and S3B), suggesting a critical role for MyD88 in the rapid production of high amounts of IFN-α/β in response to YM infection. Consistent with these data, MyD88 ablation sensitized *Ifih1*$^{-/-}$, *Mavs*$^{-/-}$, and *Tmem173*^{gt} mice to high parasitemia and host lethality (Figures 3B, S3C, and S3D). These results suggest that the rapid production of high amounts of IFN-α/β in the *Ifih1*$^{-/-}$, *Mavs*$^{-/-}$, and *Tmem173*^{gt} mice after YM infection is MyD88 dependent.

Using a similar strategy, we showed that serum amounts of IFN-α/β were very high in *Tmem173*^{gt} and *Irf3*$^{-/-}$ mice but undetectable in the sera of *Tlr7*$^{-/-}$, *Irf7*$^{-/-}$, *Tmem173*^{gt}:*Tlr7*$^{-/-}$, and *Irf3*$^{-/-}$:*Irf7*$^{-/-}$ mice (Figures 3C and 3D). TLR7 or IRF7 ablation converted the resistant phenotypes of *Tmem173*^{gt} and *Irf3*$^{-/-}$ mice to the sensitive phenotypes of *Tmem173*^{gt}:*Tlr7*$^{-/-}$ and *Irf3*$^{-/-}$:*Irf7*$^{-/-}$ mice after YM infection (Figures 3E and 3F). Similar results were observed in *Mavs*$^{-/-}$:*Tlr7*$^{-/-}$ and *Ifih1*$^{-/-}$:*Tlr7*$^{-/-}$ mice (Figures S3E and S3F). By contrast, we did not observe any difference in IFN-α/β production, parasitemia, and host death between *Ifih1*$^{-/-}$ and *Mavs*$^{-/-}$ mice versus *Ifih1*$^{-/-}$:*Tlr9*$^{-/-}$ and *Mavs*$^{-/-}$:*Tlr9*$^{-/-}$ mice (Figures S3G and S3H), indicating that TLR9 is not required for cytokine production and protective immunity. Taken together, these results suggest that TLR7-MyD88-IRF7 molecules constitute key components of MyD88-dependent type I IFN signaling, which has been shown to operate in only pDC for production of large amounts of IFN-α/β after viral infection (Liu, 2005; Wang et al., 2011).

pDCs Are the Major Source of Type I IFN Cytokine Production

To determine a role of pDCs in malaria infection, we first tested whether pDCs could be preferentially targeted by YM infection. To this end, we infected WT mice with YM and isolated cDCs, macrophages, and pDCs at 18 hr post infection to detect malaria 18S rRNA by PCR with malaria-specific primers. We found that malaria 18S rRNA could be detected in pDCs, but not in macrophages and cDCs (Figure S4A), suggesting that only pDCs are involved in detecting YM infection within the first 18 hr. To directly demonstrate that pDCs are the major source of type I IFN cytokine production, we depleted pDCs in WT, *Ifih1*$^{-/-}$, *Mavs*$^{-/-}$, and *Tmem173*^{gt} mice by injection of mPDCA-1 antibody at 12 hr before and 12 hr after YM infection. Depletion of pDCs significantly reduced serum amounts of IFN-α/β in WT and deficient mice compared with control antibody treatment (Figure 4A). Similar results were obtained in *Mb21d1*$^{-/-}$ mice (Figure S4B), suggesting that IFN-α/β are primarily produced by pDCs. Importantly, pDC depletion by mPDCA-1 treatment markedly increased parasitemias and mortality in *Ifih1*$^{-/-}$, *Mavs*$^{-/-}$, and *Tmem173*^{gt} mice infected with YM compared with control antibody-treated mice (Figures 4B and 4C). These results clearly suggest that pDCs are responsible for the early and rapid production of type I IFN in the *Ifih1*$^{-/-}$, *Mavs*$^{-/-}$, and *Tmem173*^{gt} mice, which, in turn, activates type I IFN downstream signaling for potent innate immunity against YM infection.

To further define the role of pDCs in type I IFN production and host protection after YM infection, we genetically ablated pDCs in vivo by generating *Mavs*$^{-/-}$:*BDCA2*-DTR mice, as previously described for *BDCA2*-DTR mice (Swiecki et al., 2010). Upon diphtheria toxin (DT) administration, pDCs were depleted in *Mavs*$^{-/-}$:*BDCA2*-DTR mice, but not in *Mavs*$^{-/-}$ mice. These treated mice were then infected with YM. We found that treatment of *Mavs*$^{-/-}$:*BDCA2*-DTR mice with DT markedly reduced IFN-α/β compared with DT-treated *Mavs*$^{-/-}$ mice (Figure 4D). Importantly, DT-treated *Mavs*$^{-/-}$:*BDCA2*-DTR mice were sensitive to YM infection compared with DT-treated *Mavs*$^{-/-}$ mice, which remained resistant to YM infection (Figure 4E). These results suggest that pDCs are required for robust production of type I IFN cytokines and host protective immunity against YM infection.

SOCS1 Is Induced by STING- and MAVS-Mediated Type I Signaling and Inhibits Type I IFN Signaling through MyD88

To further elucidate the mechanisms by which ablation of MDA5, MAVS, or STING markedly enhanced MyD88-dependent type I IFN production in pDCs, we hypothesized that activation of STING- and MAVS-mediated type I IFN signaling by YM may induce expression of negative regulators, which, in turn, may inhibit MyD88-dependent type I IFN signaling activation in pDCs. To test this possibility, we examined the expression pattern of several negative regulators in splenocytes from YM-infected WT and deficient mice, and found that the mRNA amounts of *Socs1*, *Socs3*, *Inpp5d* (coding for SHIP1), and *Inppl1* (coding for SHIP2) were markedly increased in WT but were little

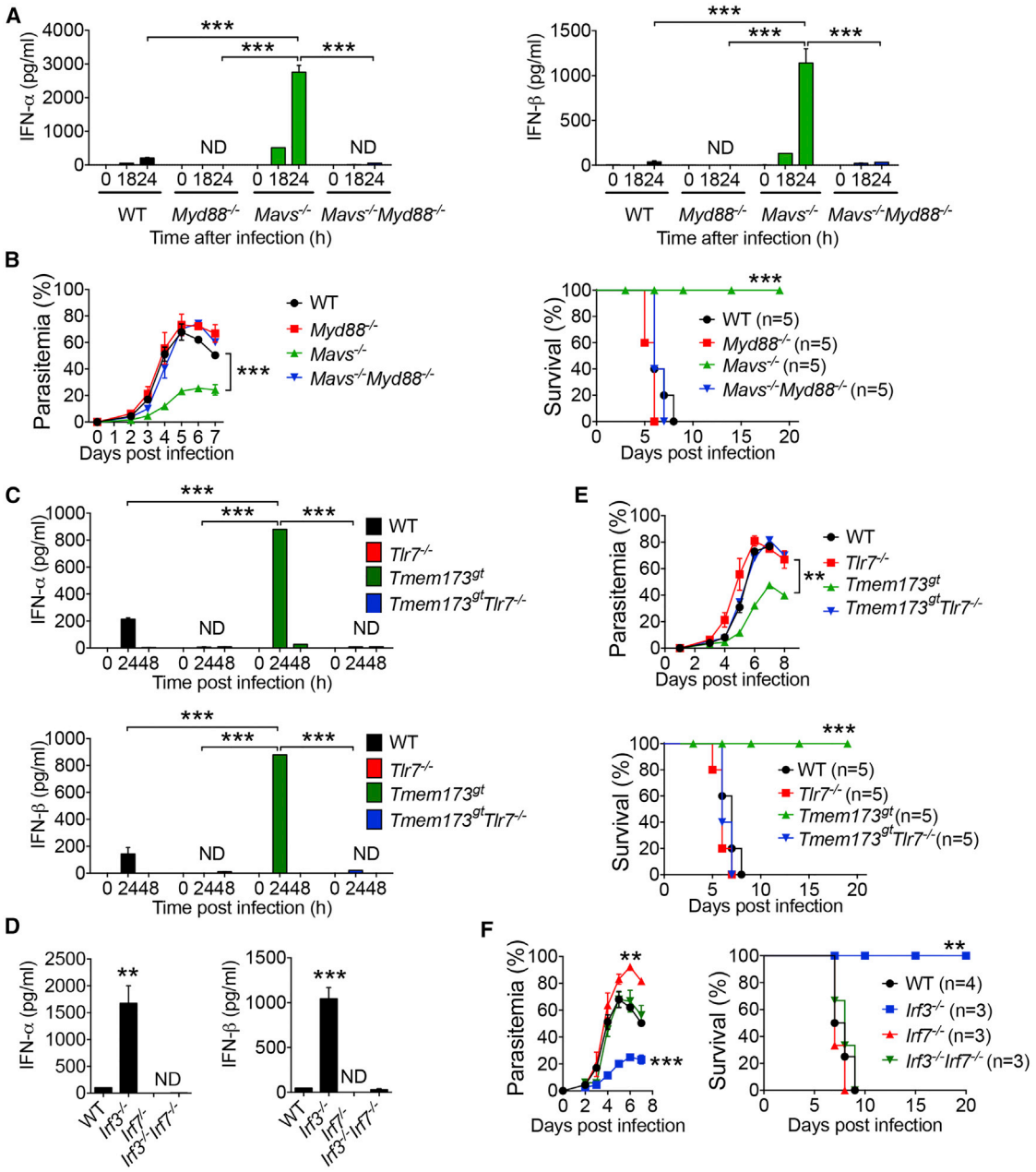

Figure 3. Requirement and Regulation of TLR7-MyD88-IRF7 in Type I IFN-Mediated Protection of Mice from YM Infection

(A) Serum amounts of IFN-α/β in WT, *Myd88*$^{-/-}$, *Mavs*$^{-/-}$, and *Mavs*$^{-/-}$:*Myd88*$^{-/-}$ mice at 0, 18, and 24 hr after YM infection.

(B) Daily YM parasitemias and mortality rates of WT, *Myd88*$^{-/-}$, *Mavs*$^{-/-}$, and *Mavs*$^{-/-}$:*Myd88*$^{-/-}$ mice after YM infection.

(C) Serum amounts of IFN-α/β in WT, *Tlr7*$^{-/-}$, *Tmem173*^{gt}, and *Tmem173*^{gt}:*Tlr7*$^{-/-}$ mice at 0, 24, and 48 hr after YM infection.

(D) Serum amounts of IFN-α/β in WT and indicated deficient mice at 24 hr after YM infection.

(E–F) Daily YM parasitemias and mortality rates of WT and indicated deficient mice after YM infection.

Data are plotted as the mean ± SD and are representative of three independent experiments. **p < 0.01, ***p < 0.001 versus corresponding control. ND, not detected.

See also Figure S3.

or low in MDA5-, MAVS-, and STING-deficient splenocytes (Figures 5A and S5A). Downregulation of *Socs1* was also observed in cGAS-deficient mice (Figure S5B). By contrast, we did not observe appreciable changes in the expression of other potential negative regulators, such as *Otud5*, *Gsk3b*, *Nlrc3*, *Pcbp2*, *Ube3c*, and *Rnf5*, between YM-infected WT and deficient mice (Figure S5A). To further assess the expression of these negative regulators in pDCs, we purified pDCs from Flt3L-induced bone-morrow-derived DCs of WT and deficient mice by flow cytometry (Figure S5C) and then stimulated them with YM RNA or gDNA.

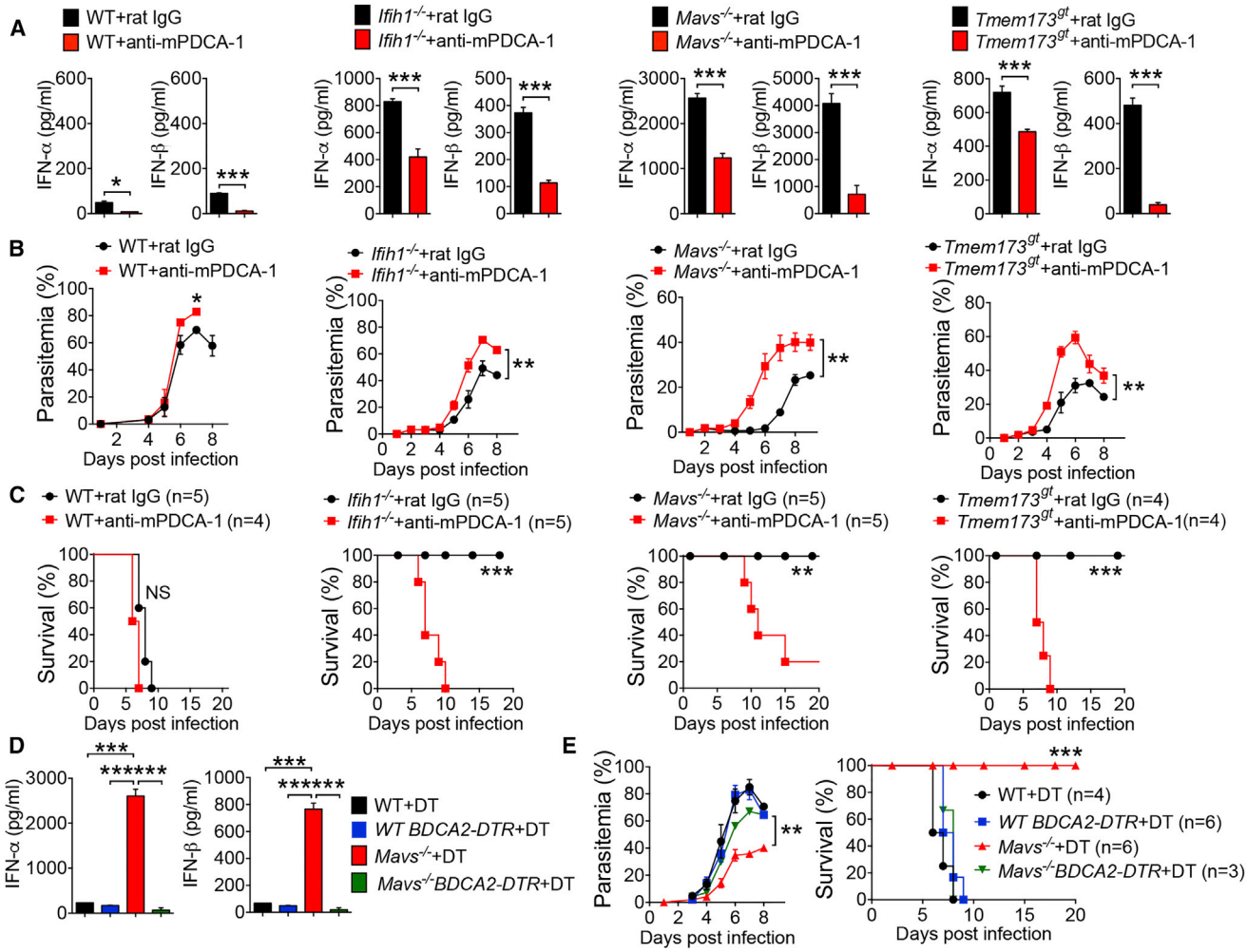

Figure 4. Requirement of Plasmacytoid DCs in Type I IFN-Mediated Protection of Mice from YM Infection

(A–C) Depletion of pDCs cell population in WT, *Ifih1*$^{-/-}$, *Mavs*$^{-/-}$, and *Tmem173*^{gt} mice by administration of anti-mPDCA-1 antibody at 12 hr before and 12 hr after YM infection. Serum amounts of IFN-α/β collected at 24 hr after infection in WT and deficient mice untreated or treated with anti-mPDCA-1 are shown in (A). Daily YM parasitemias and mortality rates are shown in (B and C).

(D and E) WT, *WT:BDCA2-DTR*, *Mavs*$^{-/-}$, and *Mavs*$^{-/-}$*:BDCA2-DTR* mice were treated with DT as indicated at 1 day before and 1, 3, and 5 days after YM infection. Serum amounts of IFN-α/β collected at 24 hr after infection are shown in (D). Daily YM parasitemias and mortality rates are shown in (E).

Data are plotted as the mean ± SD and are representative of three independent experiments. *p < 0.05, **p < 0.01, ***p < 0.001 versus corresponding control. NS, not significant.

See also Figure S4.

SOCS1 was the only negative regulator showing a marked increase in gene expression in WT pDCs but significantly lower gene expression in *Ifih1*$^{-/-}$, *Mavs*$^{-/-}$, and *Tmem173*^{gt} pDCs (Figures 5B and 5C). No appreciable differences in expression of other negative regulators *Socs3*, *Inpp5d*, and *Inppl1* were observed between WT and deficient pDCs after YM RNA or gDNA stimulation (Figure S5D). To further substantiate these findings, we purified pDCs, macrophages, and cDCs from YM-infected WT and *Mavs*$^{-/-}$ mice (18 hr after infection) and then directly assessed SOCS1 expression in these cells, and we found that SOCS1 mRNA abundance in pDCs from WT mice were significantly higher than pDCs from *Mavs*$^{-/-}$ mice (Figure 5D). Notably, we did not detect any difference in expression of SOCS1 in macrophages and cDCs from WT and *Mavs*$^{-/-}$ mice (Figure 5D). Importantly, SOCS1 mRNA abundance was inversely correlated with IFN-α/β mRNA and protein expression in pDCs from YM-infected WT and *Mavs*$^{-/-}$ mice (Figures 5E and 5F). Similar results were obtained using purified pDCs, cDCs, and macrophages treated in vitro with YM-iRBCs (Figures S5E and S5F).

Next, we determined how SOCS1 inhibits MyD88-dependent type I IFN signaling. Although previous studies showed that SOCS1 inhibits the NF-κB signaling pathway by interacting with IRAK1 (Nakagawa et al., 2002), the involvement of SOCS1 in MyD88-mediated type I IFN signaling is not known. To determine whether SOCS1 directly interacts with MyD88, we performed co-immunoprecipitation of 293T cells expressing *Socs1* plus *Myd88*, *Irak1*, or *Irak4*, and we found that SOCS1

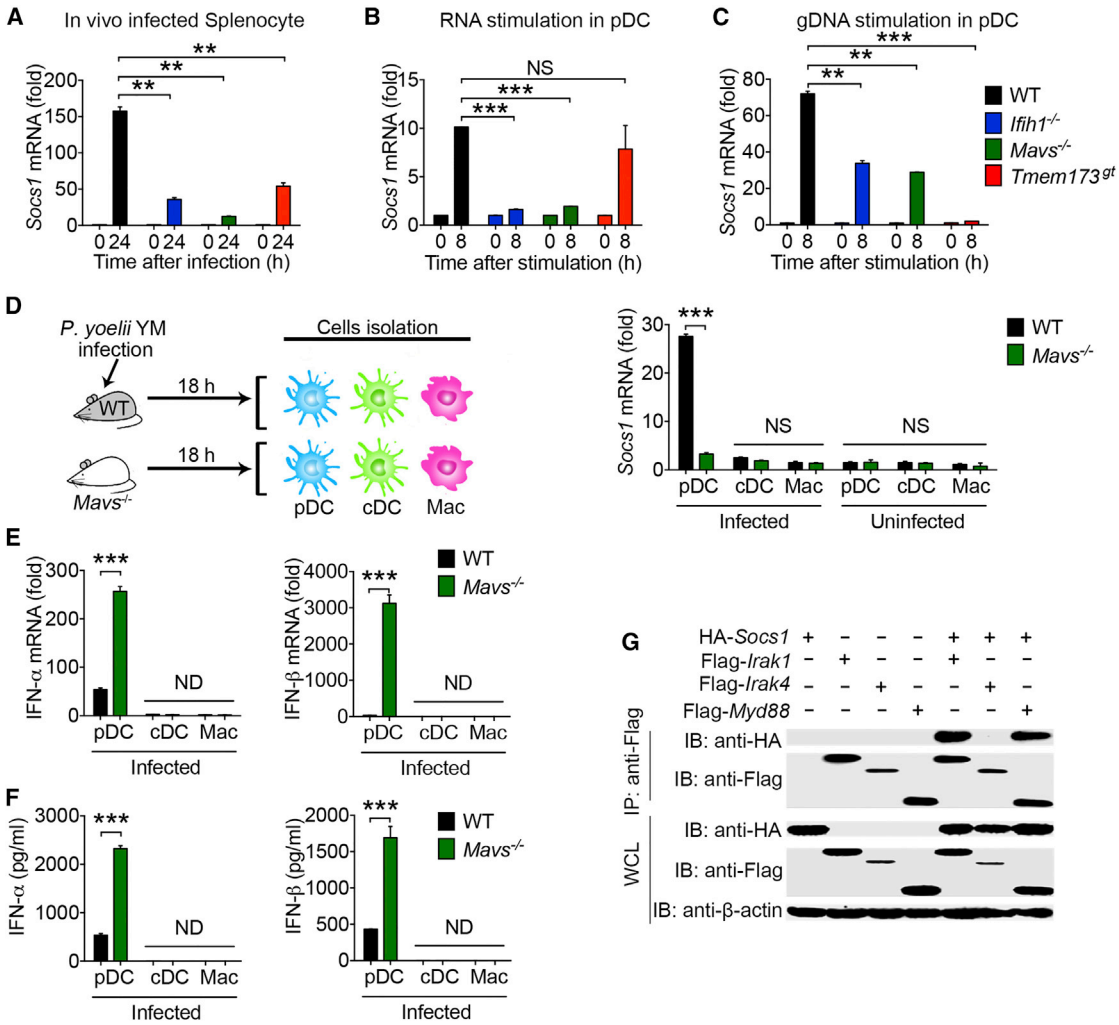

Figure 5. SOCS1 Is a Key Negative Regulator Induced by STING- and/or MAVS-Mediated Signaling and Inhibits Type I IFN Signaling through MyD88 in pDCs

(A) Expression of negative regulators *Socs1* in the spleens of WT and deficient (*Ifih1*$^{-/-}$, *Mavs*$^{-/-}$, and *Tmem173*^{gt}) mice at the indicated time points after YM infection. RNAs from splenocytes were isolated and used for expression analysis.

(B and C) Expression of *Socs1* in pDCs of WT and deficient (*Ifih1*$^{-/-}$, *Mavs*$^{-/-}$, and *Tmem173*^{gt}) mice after YM RNA (B) or gDNA (C) stimulation.

(D) WT and *Mavs*$^{-/-}$ mice were infected with YM for 18 hr. pDCs, cDCs, and macrophages were isolated and purified from infected mice and used for analysis of *Socs1* mRNA expression by qPCR.

(E and F) IFN-α/β expression at the mRNA (E) and protein (F) amounts in pDCs, cDCs, or macrophages from WT and *Mavs*$^{-/-}$ mice after overnight culture.

(G) SOCS1 interacts with MyD88 and IRAK1. 293T cells were transfected with HA-*Socs1* and Flag-*Irak1*, Flag-*Irak4*, or Flag-*Myd88*. Immunoprecipitation was performed with an anti-Flag, followed by immunoblotting with an anti-HA or anti-Flag antibody. Whole-cell lysates were immunoblotted for protein expression.

Data are plotted as the mean ± SD and are representative of three independent experiments. **p < 0.01, ***p < 0.001 versus corresponding control. NS, not significant. ND, not detected.

See also Figures S5 and S6.

directly interacted with MyD88 (Figure 5G), in addition to IRAK1. To determine whether STING-, MDA5-, and MAVS-induced SOCS1 are responsible for inhibition of MyD88-dependent type I IFN production in pDCs, we silenced *Socs1*, *Socs3*, *Inpp5d*, and *Inppl1* in WT pDCs by siRNA transfection (Figure S6A) and then determined IFN-α/β production after YM RNA and gDNA stimulation. Only silencing of *Socs1* resulted in a significant increase in IFN-α/β mRNA, as well as IFN-β protein after YM RNA and gDNA stimulation (Figures S6B and S6C), suggesting that STING- or MAVS-mediated type I IFN signaling induces SOCS1 expression, which, in turn, inhibits MyD88-dependent type I IFN production in pDCs.

SOCS1-Mediated Inhibition of Type I IFN Signaling Is pDC Specific and MyD88 Dependent

Next, we sought to determine the role of SOCS1 in inhibiting MyD88-mediated type I IFN production and protective immunity in vivo. Due to neonatal mortality and the complex inflammatory pathology of *Socs1*$^{-/-}$ mice, the in vivo role of SOCS1 in response to malaria infection could not be addressed. Hence,

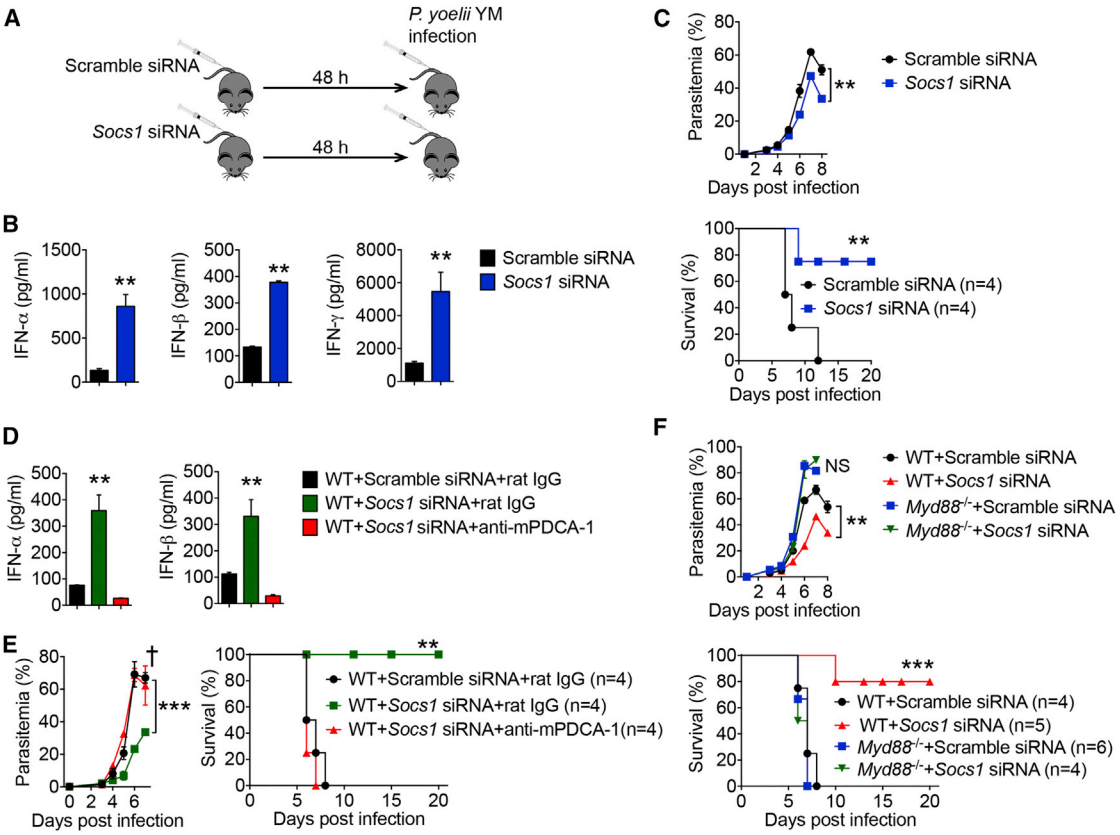

Figure 6. SOCS1 Is Responsible for Inhibition of Myd88-Dependent Type I IFN in pDCs

(A–C) C57BL/6 mice were treated with *Socs1*-specific or scramble siRNA for 48 hr, followed by YM (0.5×10^6 iRBCs) infection. Diagram of experiment procedure are shown in (A). Serum amounts of IFN-α/β and IFN-γ in *Socs1*-specific or scrambled siRNA-treated mice at 24 hr after YM infection are shown in (B). Daily YM parasitemias and mortality rates are shown in (C).

(D and E) WT mice were treated with scramble siRNA, *Socs1*-specific siRNA, or *Socs1*-specific siRNA with anti-mPDCA-1 antibody at 24 hr before infection, followed by YM (0.5×10^6 iRBCs) infection. Serum amounts of IFN-α/β collected at 24 hr after infection are shown in (D). Daily YM parasitemias and mortality rates are shown in (E).

(F) WT and *Myd88*$^{-/-}$ mice were treated with *Socs1*-specific or scramble siRNA for 48 hr, followed by YM (0.5×10^6 iRBCs) infection. Daily YM parasitemias and mortality rates are shown.

Data are plotted as the mean ± SD and are representative of three independent experiments. **p < 0.01, ***p < 0.001 versus corresponding control. NS, not significant.

See also Figure S6.

we first silenced the *Socs1* gene in WT mice with *Socs1*-specific siRNA (Figures 6A and S6D). As expected, silencing of *Socs1* increased IFN-γ production through its inhibitory effect on JAK1. We also found increased serum amounts of IFN-α/β compared with scrambled siRNA-treated WT mice after YM infection (Figure 6B). Importantly, silencing of *Socs1* resulted in reduction of parasitemia and increased survival of WT mice after YM infection compared with control mice (Figure 6C). To further confirm these observations, we genetically ablated the *Socs1* gene in WT bone marrow cells using the CRISPR/Cas9 system, and then we generated chimeric mice (Figures S6E and S6F). SOCS1-deficient chimeric mice produced high amounts of IFN-α/β, reduced parasitemia, and increased survival after YM infection (Figures S6G and S6H). These results suggest that silencing or genetic deletion of *Socs1* relieves its inhibition of the MyD88-dependent type I IFN signaling pathway, thus leading to the control of parasitemia and host survival.

To provide direct evidence that SOCS1-mediated inhibition of MyD88-dependent type I IFN signaling is pDC-specific, we silenced *Socs1* in WT mice at 24 hr before infection with or without pDC depletion using anti-mPDCA-1. We showed that the high serum amounts of IFN-α/β observed in *Socs1*-silenced mice were abolished upon pDC depletion (Figure 6D). Consistently, pDC depletion in *Socs1*-silenced mice also increased parasitemia and host mortality after infection compared with *Socs1*-silenced mice without pDC depletion (Figure 6E). These results suggest that SOCS1-mediated inhibition of MyD88-dependent type I IFN signaling is pDC specific.

Because SOCS1 can inhibit MyD88-dependent type I IFN signaling (as presented in this study) and JAK1 in STAT signaling (a downstream IFN-stimulated signaling pathway for IFN-γ production) (Figure S6I), we determined whether SOCS1-mediated type I IFN signaling inhibition is MyD88-dependent. As expected, *Socs1*-silenced mice reduced parasitemia and

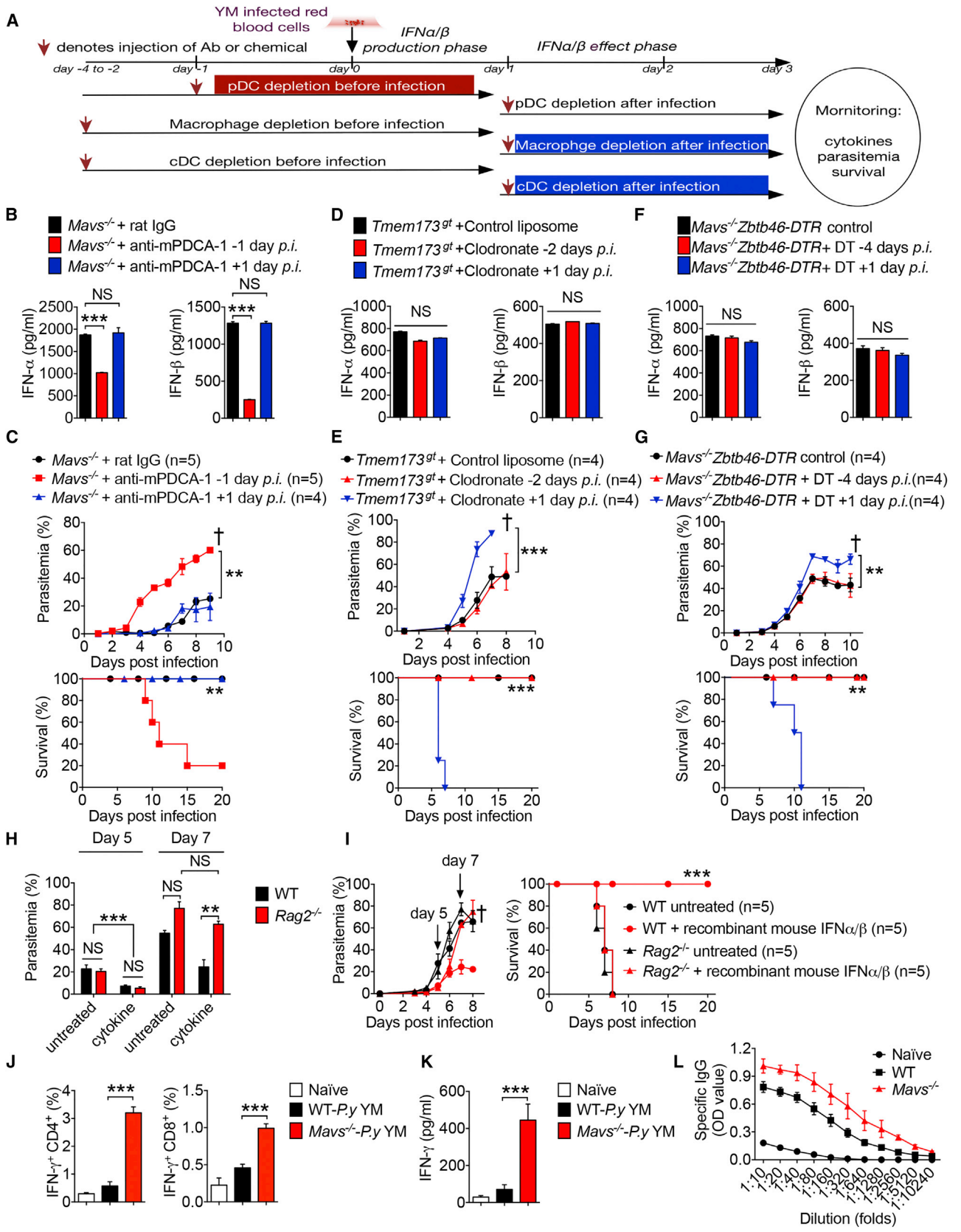

(legend on next page)

increased survival after YM infection. By contrast, *Myd88*$^{-/-}$ mice with *Socs1* silencing did not show reduced parasitemia or increased survival compared with those treated with scrambled siRNA (Figure 6F). Consistently, we could not detect any IFN-α/β in *Myd88*$^{-/-}$ mice regardless of *Socs1* silencing, indicating that SOCS1-mediated type I IFN signaling inhibition is MyD88 dependent (Figure S6J). Taken together, these results suggest that SOCS1, which is induced by the STING and/or MAVS pathways in response to YM infection, mainly inhibits MyD88-dependent type I IFN signaling and host survival.

pDCs, Macrophages, and cDCs Are Required in a Stage-Specific Manner for Generating IFN-α/β-Induced Protective Immunity against YM Infection

To understand how the early burst of type I IFN-α/β production in pDCs induces subsequent protective immunity and whether macrophages and cDCs are required for inducing potent immunity against YM infection, we depleted specific cell populations in different phases and then determined their contribution to cytokine production, parasitemia, and host survival (Figure 7A). We found that depletion of pDCs with anti-mPDCA-1 in *Mavs*$^{-/-}$ mice during the cytokine production phase (24 hr before infection) markedly reduced IFN-α/β production; however, depletion of pDCs after 24 hr of infection had no effect on IFN-α/β production compared with mice treated with a control antibody (Figure 7B). Consistently, *Mavs*$^{-/-}$ mice treated with anti-mPDCA-1 during the cytokine production phase had increased parasitemia and host mortality but had no change in parasitemia and host survival when treated with anti-mPDCA-1 in the effector phase compared with control antibody-treated mice (Figure 7C). Collectively, these results clearly demonstrate the importance of pDCs in the production of IFN-α/β within the first 24 hr, but not after 24 hr of infection, for the protective immunity.

To determine the importance of macrophages in cytokine production, parasitemia, and host mortality, we depleted macrophages with clodronate at 2 days before or 1 day after YM infection (Figure S7A). Macrophage depletion in *Tmem173*^{gt} mice did not affect serum amounts of IFN-α/β, regardless of depletion at 2 days before or 1 day after YM infection (Figure 7D). However, macrophage depletion during the effector phase (at 1 day post infection) markedly increased parasitemia and host mortality compared with a liposome control or treatment at 2 days before infection (Figure 7E), suggesting a critical role of macrophages during the effector phase, but not during the cytokine production phase. To determine the relative role of cDCs in anti-malaria immunity, we generated *Mavs*$^{-/-}$:*Zbtb46-DTR* (zinc figure transcription factor-driven DTR expression in cDCs) mice. As expected in a previous study (Meredith et al., 2012), DT injection into *Zbtb46-DTR* bone marrow chimeras resulted in specific depletion of cDCs in 12 hr and maintained depletion for 5 days. Thus, we injected DT into *Mavs*$^{-/-}$:*Zbtb46-DTR* chimeric mice at 4 days before or at 1 day post infection. We found that there was no change in the serum amounts of IFN-α/β when DT was injected either before or after YM infection (Figure 7F), suggesting that cDCs are not responsible for the IFN-α/β production during the early phase (24 hr) of infection. However, *Mavs*$^{-/-}$:*Zbtb46-DTR* mice treated with DT after 24 hr of infection showed increased parasitemia and died sooner after infection compared to untreated mice or mice treated with DT at 4 days before infection (Figure 7G), suggesting that cDCs are required for generating protective immunity during the effector phase. Consistent with these results, we also found that malaria 18S rRNA could be detected in pDCs, but not in macrophages or cDCs, at 18 hr post infection. However, malaria 18S rRNA could be detected in macrophages and cDCs of *Mavs*$^{-/-}$ mice at day 3 post infection (Figure S7B), suggesting that pDCs are the major cell population that sense and detect YM infection within the first 24 hr, whereas macrophages and cDCs are involved in the detection of YM infection at later time points for the induction of adaptive immunity. Taken together, these results suggest that pDCs, but not macrophages or cDCs, are critically required for the production of IFN-α/β in the first 24 hr after YM infection, whereas macrophages and cDCs are required for IFN-α/β-induced immunity against YM after 24 hr post infection.

Next, we determined whether B and T cells are required for IFN-α/β-induced immunity against YM, in particular for clearing malaria in the late phase of infection. To test this possibility, we infected WT and Rag2-deficient mice, which lack B and T cells, with YM in the presence or absence of exogenous murine recombinant IFN-α/β. Although cytokine-treated WT and *Rag2*$^{-/-}$ mice demonstrated reduced parasitemia compared with untreated WT and *Rag2*$^{-/-}$ mice, we found no differences

Figure 7. Stage-Specific Role of pDCs, Macrophages, and cDCs in Generating IFN-α/β-Induced Protective Immunity

(A) Schematic figure to show cell depletion at different stages of IFN-α/β cytokine production after YM infection.

(B and C) Depletion of pDCs in *Mavs*$^{-/-}$ mice by anti-mPDCA-1 antibody administrated at 24 hr before or 24 hr after YM infection. Serum amounts of IFN-α/β collected at 24 hr after infection are shown in (B). Daily YM parasitemias and mortality rates are shown in (C).

(D and E) Depletion of macrophages in *Tmem173*^{gt} mice by clodronate (700 μg/injection) administered 2 days before or 1 day after YM infection. Control liposome served as a control. Serum amounts of IFN-α/β collected at 24 hr after YM infection in *Tmem173*^{gt} mice untreated (control liposome) or treated with clodronate at the indicated times are shown in (D). Parasitemias and mortality rates are shown in (E).

(F and G) WT chimeric mice were irradiated and transplanted with bone marrow cells of *Mavs*$^{-/-}$:*Zbtb46-DTR* mice, then untreated or treated with DT as indicated at 4 days before or 1 day after YM infection. Serum amounts of IFN-α/β collected at 24 hr after infection are shown in (F), and daily YM parasitemias and mortality rates are shown in (G).

(H and I) WT and *Rag2*$^{-/-}$ mice were infected with YM, followed by i.v. administration of recombinant mouse IFN-α/β at 18 hr post infection. Parasitemias at day 5 and day 7 are shown in (H). Daily YM parasitemias and mortality rates are shown in (I).

(J and K) Intracellular staining of IFN-γ were measured by flow cytometry in splenocytes of WT and *Mavs*$^{-/-}$ mice at day 10 post YM infection, followed by stimulation with crude antigens (YM iRBCs). Statistical analysis is shown in (J). Meanwhile, splenocytes from YM-infected WT and *Mavs*$^{-/-}$ mice were cultured with crude antigens (iRBCs) overnight, and cell supernatants were collected for ELISA analysis (K).

(L) Malaria specific IgG in serum from WT and *Mavs*$^{-/-}$ mice at day 10 post YM infection, evaluated by ELISA.

Data are representative of three independent experiments and are plotted as the mean ± SD. *$p < 0.05$, **$p < 0.01$, ***$p < 0.001$ versus corresponding control. NS, not significant. † denotes mouse death.

See also Figure S7.

in the percent of parasitemia between WT and *Rag2*$^{-/-}$ mice either in untreated groups or cytokine-treated groups in the first 5 days after infection (Figure 7H). However, after 7 days post infection, parasitemia in cytokine-treated *Rag2*$^{-/-}$ mice markedly increased to the amounts observed in untreated WT or untreated *Rag2*$^{-/-}$ mice (Figures 7H and 7I). WT untreated, *Rag2*$^{-/-}$ untreated, and *Rag2*$^{-/-}$ cytokine-treated mice died within 8 days after YM infection, whereas cytokine-treated WT mice maintained significantly lower parasitemia than the other three groups and survived beyond 8 days (Figure 7I), suggesting that B and T cells are required for generating adaptive immunity to control parasitemia and clear parasites at a later time. To further understand cellular and molecular basis of YM-induced adaptive immunity in WT and *Mavs*$^{-/-}$ mice, we infected WT and *Mavs*$^{-/-}$ mice with 0.1 × 10^6 YM iRBCs (10 times lower dosage to keep WT mice alive) and isolated splenocytes at day 10 post infection, then we stimulated with crude antigen (*P.y* YM-iRBC) for T and B cells function analysis. Our results showed that the percentage of splenic IFN-γ^+ CD4$^+$ and IFN-γ^+ CD8$^+$ cells from *Mavs*$^{-/-}$ mice were much higher than those from WT mice (Figure 7J). Consistently, IFN-γ protein amounts in the supernatant of splenocytes after overnight culture with crude antigens and concentrations of malaria-specific immunoglobulin G (IgG) in serum were significantly higher in *Mavs*$^{-/-}$ mice than in WT mice (Figures 7K and 7L), suggesting that YM-infected *Mavs*$^{-/-}$ mice developed much stronger adaptive (B and T cell) immune responses than WT mice.

DISCUSSION

Our study shows that cGAS functions as a DNA sensor for recognizing malaria gDNA and triggers STING-mediated type I IFN signaling. STING-deficient mice were more resistant to YM infection than were cGAS-deficient mice, suggesting that other DNA sensors might function in recognizing malarial genomic DNA. For RNA sensing, MDA5, but not RIG-I, is responsible for detecting malaria RNA and triggers MAVS-mediated type I IFN signaling. It is known that RIG-I recognizes RNA with a triphosphate (PPP) moiety and 5′ blunt-ended 20 nucleotides, whereas MDA5 recognizes long dsRNA (1–2 kb) (Goubau et al., 2013). These structural and length requirements of dsRNA may explain why malaria RNA interacts with MDA5, but not with RIG-I, to trigger downstream MAVS-dependent type I IFN signaling. Although cGAS-STING- and MDA5-MAVS-mediated type I IFN signaling is important and operates in all cell types, including macrophages and cDCs, we did not detect YM malaria 18S rRNA or observe IFN-β and SOCS1 expression in macrophages and cDCs within the first 18–24 hr post infection. Depletion of macrophages or cDCs did not affect the production of IFN-α/β at 24 hr post infection, further suggesting that macrophages and cDCs are not involved the production of IFN-α/β in the early stage of YM infection.

To understand high serum amounts of IFN-α/β in *Ifih1*$^{-/-}$, *Mavs*$^{-/-}$, *Tmem173*^{gt}, or *Mb21d1*$^{-/-}$ mice, we have provided several lines of evidence to support our conclusion: (1) *Ifih1*$^{-/-}$:*Myd88*$^{-/-}$, *Mavs*$^{-/-}$:*Myd88*$^{-/-}$, or *Tmem173*^{gt}:*Myd88*$^{-/-}$ mice failed to produce any IFN-α/β and become susceptible to YM infection, compared with *Ifih1*$^{-/-}$, *Mavs*$^{-/-}$, and *Tmem173*^{gt} mice; (2) depletion of pDCs by a specific antibody or genetic ablation markedly reduced the production of IFN-α/β, suggesting that pDCs are the major sources for production of these cytokines. Thus, our results provide direct evidence that MyD88-dependent type I IFN signaling in pDCs plays a critical role in the early production of IFN-α/β and protection against malaria infection.

To identify the mechanisms and sequential order of immune responses induced by IFN-α/β-producing pDCs, we depleted pDCs, macrophages, cDCs, or T cells at different times and determined their roles in the production of IFN-α/β, parasitemia, and host survival. Our results clearly demonstrate the requirement for pDCs in the production of IFN-α/β during the first 24 hr of infection, but not after that time. Conversely, depletion of macrophages or cDCs during the first 24 hr of infection affected neither IFN-α/β production nor parasitemia or host mortality in this YM model. However, depletion of macrophages or cDCs after 24 hr post infection resulted in increased parasitemia and host mortality, suggesting that these cell types participated in anti-malaria immunity, which is consistent with previous results showing that classic DCs are required for inducing T cell response (Voisine et al., 2010). Although B cells and T cells are not required for IFN-α/β production and parasitemia control during the first 5–6 days post infection, they are required for the control of parasitemia and host mortality at later times (>6 days), as suggested by previous studies using cerebral malaria (Ball et al., 2013; Haque et al., 2014).

We have shown that TLR7, but not TLR9, was essential for IFN-α/β production in pDCs. YM RNA activates TLR7 and recruits the downstream adaptor MyD88 to trigger IRF7-mediated type I IFN signaling pathway. However, previous studies show that mice deficient with STING, TBK1, IRF3 and IRF7, or IFNAR1 expression are resistant to *P. berghei* ANKA infection (Haque et al., 2014; Sharma et al., 2011), suggesting that type I IFN impairs host anti-malaria responses to ANKA. To explain why type I IFN plays opposing roles in host immune responses to different malaria strain infection, we examined the timing and amounts of IFN-α/β production in response to two lethal *Plasmodium* strains (*P. yoelii* YM and *P. berghei* ANKA) and found that the timing and amounts of IFN-α/β production are different in WT mice in response to YM or ANKA infection: low amount of IFN-α/β only at day 1 after YM infection versus large amounts of IFN-α/β at day 4 after ANKA infection (Haque et al., 2014). We propose that early robust production or administration of type I IFN (18–24 hr post infection) is essential to induce innate and adaptive immunity against malaria. By contrast, late time production of type I IFN (3–4 days after ANKA infection) impairs host anti-malaria immune responses. Thus, different malaria strains have evolved to evade host immune system by either inhibiting type I IFN production at the early infection phase (in YM strain) or shifting type I IFN production to the late time (4 days post infection) (in ANKA strain). Similar results have been obtained in LCMV infection or other pathogens (O'Connell et al., 2004; Teles et al., 2013; Wilson et al., 2013). In these cases, persistent production of type I IFN even at day 9 post LCMV infection is observed, which, in turn, induces the expression of negative regulators, such as IL-10 and PD-L1, to inhibit adaptive immune response. Our study showed that robust type I IFN production (only at day 1) produced by pDCs activates cDCs and macrophages to induce adaptive immune response for the clearance of YM infection.

Our notion is also supported by a recent study, showing that administration of type I IFN at an early time (6–12 hr post-infection) after SARS-CoV infection promotes host innate and adaptive immune response. By contrast, delayed type I IFN production promotes lung immunopathology with diminished survival and impairs anti-viral immunity (Channappanavar et al., 2016). Thus, early robust production of type I IFN (18–24 hr post infection) promotes innate and adaptive immune responses, while delayed type I IFN production (3–4 days post infection) impairs innate and adaptive immune responses. The timing and amounts of type I IFN production may be dependent upon cell tropism (targeting different cell types during infection) and distinct strain-specific pathogenesis (Gun et al., 2014; Wu et al., 2014). Further studies are needed to understand the molecular mechanisms responsible for these opposing roles of type I IFN in malaria and viral infection.

Our study identified SOCS1 as a key negative regulator, which interacted with MyD88 and inhibited MyD88-dependent type I IFN signaling. A recent study shows a role for STING in negatively regulating inflammatory responses of macrophages in systemic lupus erythematosus (SLE) through upregulation of A20, SOCS1, and SOCS3 (Sharma et al., 2015), but its role in MyD88-dependent type I IFN signaling is not known in this disease model. We further showed that inactivation of *Ifih1*, *Tmem173*, or *Mavs* markedly reduced *Socs1* expression in vitro and in vivo and increased IFN-α/β mRNA and protein expression. Silencing or genetic deletion of *Socs1* in YM-infected WT mice markedly reduced parasitemia and host mortality. The predominant role of SOCS1 is to regulate MyD88-dependent type I IFN signaling in pDCs because the observed increase in IFN-α/β expression after siRNA-mediated *Socs1* silencing disappeared when pDCs were depleted, suggesting that *Socs1* silencing mainly affects MyD88-dependent type I IFN signaling in pDCs. Based on these findings, we propose a working model to illustrate how type I IFN is regulated in response to YM infection (Figure S7C). Activation of cGAS-STING and MDA5-MAVS by YM infection triggers IRF3-mediated type I IFN signaling in pDCs, which produce low amounts of IFN-α/β and activate negative regulator SOCS1 in WT pDCs. SOCS1 then inhibits MyD88-dependent type I IFN signaling pathway, which produces more than 100-fold higher cytokine amounts than those produced by STING- and MAVS-mediated IRF3-dependent type I IFN signaling pathway. By contrast, SOCS1 expression is markedly reduced in $Ifih1^{-/-}$, $Mavs^{-/-}$, and $Tmem173^{gt}$ pDCs, allowing the activation of MyD88-dependent type I IFN signaling. Thus, lethal YM infection activates two distinct type I IFN signaling pathways in pDCs. YM takes advantage of the cross-inhibition of TLR7-MyD88-mediated type I IFN signaling by cGAS-STING- and MDA5-MAVS-mediated type I IFN through upregulation of *Socs1* in WT mice to avoid host innate immune response. Silencing or genetic ablation of genes, such as *Socs1* or those in the STING- and MAVS-mediated type I IFN signaling pathway, relieves SOCS1-suppressive effects on TLR7-MyD88-mediated type I IFN signaling and permits robust production of IFN-α/β in the first 24 hr post infection, then activates downstream signaling pathways via IFNAR in other innate immune cells, such as macrophages and cDCs, for priming adaptive immunity mediated by B and T cells to clear YM infection at later times. Thus, our findings not only identify a critical regulatory mechanism between different type I IFN signaling pathways in pDCs, as well as a critical role of stage-dependent type I IFN production and specific contribution of different immune cells for developing protective immunity, but also provide potential therapeutic targets for the development of safe and effective malaria vaccines.

EXPERIMENTAL PROCEDURES

Malaria Parasites and Mice

The parasite YM has been previously described (Li et al., 2011). For YM infection, 1×10^6 iRBCs (otherwise indicated specifically in the figure legend) suspended in 200 μL PBS from the donor mice were injected i.p. into experimental mice. All mouse-related procedures were performed according to experimental protocols approved by the Animal Care and Welfare Committee at Houston Methodist Research Institute and in accordance with NIH-approved animal study protocol LMVR-11E. See Supplemental Experimental Procedures for more details of this and following sections.

Antibody Treatments

To block type I IFN receptor, anti-mouse IFN-α/β receptor antibodies, in the amount of 500 μg in PBS at day 0, 2, 4, and 250 μg at day 6 after infection, were injected i.p. into WT and deficient mice. To deplete pDCs, pDC-depleting functional-grade mAb (anti-mPDCA-1 IgG) and the corresponding isotype control IgG served as control and were purchased from Miltenyi Biotec, and two i.p. injections of antibody (250 μg/mouse) per mouse were administered 12 hr prior and after YM infection.

Isolation and Purification of Immune Cell Populations

Bone marrow cells were isolated from the tibia and femur and cultured in RPMI1640 medium with 10% FBS, 1% penicillin-streptomycin, 55 μM β-mercaptoethanol, and 10% L929 conditioned media containing macrophage-colony stimulating factor for 5 days for BMDMs, 20 ng/mL murine GM-CSF and 10 ng/ml IL-4 for 6–8 days for cDCs, and 200 ng/mL Flt3L for pDCs. pDCs were further purified by flow cytometry analysis gating on $CD11b^{-}B220^{+}$ $CD11c^{+}$ cell population.

RNAi-Mediated Silencing in Mice

In vivo ready siRNAs were mixed with invivofectamine 2.0 liposomes (Invitrogen) following the manufacturer's instructions and injected intravenously (i.v.) in a volume of 100 μL at a dose of 5 mg/kg. Mice were infected with YM (0.5×10^6 iRBCs) 48 hr after siRNA treatment.

RNA Preparation and qPCR

Total RNA was harvested from splenic tissue or stimulated cells using the TRIzol reagent, and the complimentary cDNA was generated using reverse transcriptase III. Real-time PCR was carried out using the ABI Prism 7000 analyzer using the SYBR GreenER qPCR Super Mix Universal and specific primers.

Diphtheria Toxin Treatment

$Ifih1^{-/-}$, $Mavs^{-/-}$, and $Tmem173^{gt}$ mice were crossed with *BDCA2-DTR* transgenic mice to generate $Ifih1^{-/-}$: *BDCA2-DTR*, $Mavs^{-/-}$:*BDCA2-DTR* and $Tmem173^{gt}$:*BDCA2-DTR* mice, respectively, and then treated with diphtheria toxin (DT) i.p. at dose of 100–120 ng/mouse. pDCs were depleted by DT injection at 1 day before and 1, 3, and 5 days after YM infection. For cDC depletion, bone marrow chimeras were reconstituted for at least 6–8 weeks after lethal irradiation (950 cGy) and i.v. transferred with 10×10^6 bone marrow cells from $Mavs^{-/-}$:*Zbtb46-DTR* mice and then injected with DT at a dose of 2.5 ng per gram of body weight.

ELISA

Mouse serum or cell supernatants were collected at the indicated time after infection or stimulation and subjected to analysis with commercial ELISA kits for mouse IFN-α, IFN-β (PBL Biomedical Laboratories), IL-6, or IFN-γ (eBioscience) following the manufacturer's instructions.

Statistical Analysis

All analyses were performed using GraphPad Prism version 5.0 (GraphPad Software, La Jolla, CA). Data are presented as means ± SD unless otherwise stated. Statistical significance of differences between two groups was assessed by unpaired Student's *t* tests and a p value of <0.05 was considered significant.

SUPPLEMENTAL INFORMATION

Supplemental Information includes Supplemental Experimental Procedures and seven figures and can be found with this article online at http://dx.doi.org/10.1016/j.immuni.2016.10.001.

AUTHOR CONTRIBUTIONS

X.Y., B.C., and M.W. performed the experiments. P.T., X.D., Q.L., P.L., C.X., and J.L. provided assistance or technique support in some experiments. J.W. and X.-Z.S. provided malaria strains and some experimental assistance. X.Y., H.Y.W., X.-Z.S., and R.-F.W. performed data analysis and wrote the manuscript. R.-F.W. supervised the entire project and designed experiments.

ACKNOWLEDGMENTS

We thank Marco Colonna (Washington University School of Medicine) for providing *Tlr9*$^{-/-}$ mice, Richard A. Flavell (Yale University) for *Tlr7*$^{-/-}$ mice, Kate Fitzgerald (University of Massachusetts Medical School) and Tadatsugo Taniguchi (The University of Tokyo) for *Irf3*$^{-/-}$:*Irf7*$^{-/-}$ mice, Michael Gale (University of Washington) and Wenxin Wu (University of Oklahoma Health Science Center) for *Ddx58*$^{-/-}$ mice, and Skip Virgin (Washington University at St. Louis) for *Mb21d1*$^{-/-}$ mice, Bo Ning for art drawing, and Jana S. Burchfield for editing the manuscript. X.Y. and B.C. were partially supported by the China Scholar Council. This work was supported, in part, by grants (R01CA101795 and DA030338) from the NCI and NIDA, NIH to R.-F.W. and by the Division of Intramural Research at the National Institute of Allergy and Infectious Diseases (NIAID).

Received: April 15, 2016
Revised: August 5, 2016
Accepted: August 22, 2016
Published: October 25, 2016

REFERENCES

Baccarella, A., Fontana, M.F., Chen, E.C., and Kim, C.C. (2013). Toll-like receptor 7 mediates early innate immune responses to malaria. Infect. Immun. *81*, 4431–4442.

Ball, E.A., Sambo, M.R., Martins, M., Trovoada, M.J., Benchimol, C., Costa, J., Antunes Gonçalves, L., Coutinho, A., and Penha-Gonçalves, C. (2013). IFNAR1 controls progression to cerebral malaria in children and CD8+ T cell brain pathology in Plasmodium berghei-infected mice. J. Immunol. *190*, 5118–5127.

Channappanavar, R., Fehr, A.R., Vijay, R., Mack, M., Zhao, J., Meyerholz, D.K., and Perlman, S. (2016). Dysregulated Type I Interferon and Inflammatory Monocyte-Macrophage Responses Cause Lethal Pneumonia in SARS-CoV-Infected Mice. Cell Host Microbe *19*, 181–193.

Gazzinelli, R.T., Kalantari, P., Fitzgerald, K.A., and Golenbock, D.T. (2014). Innate sensing of malaria parasites. Nat. Rev. Immunol. *14*, 744–757.

Goubau, D., Deddouche, S., and Reis e Sousa, C. (2013). Cytosolic sensing of viruses. Immunity *38*, 855–869.

Gowda, N.M., Wu, X., and Gowda, D.C. (2012). TLR9 and MyD88 are crucial for the development of protective immunity to malaria. J. Immunol. *188*, 5073–5085.

Gun, S.Y., Claser, C., Tan, K.S., and Rénia, L. (2014). Interferons and interferon regulatory factors in malaria. Mediators Inflamm. *2014*, 243713.

Haque, A., Best, S.E., Ammerdorffer, A., Desbarrieres, L., de Oca, M.M., Amante, F.H., de Labastida Rivera, F., Hertzog, P., Boyle, G.M., Hill, G.R., and Engwerda, C.R. (2011). Type I interferons suppress CD4^{+} T-cell-dependent parasite control during blood-stage Plasmodium infection. Eur. J. Immunol. *41*, 2688–2698.

Haque, A., Best, S.E., Montes de Oca, M., James, K.R., Ammerdorffer, A., Edwards, C.L., de Labastida Rivera, F., Amante, F.H., Bunn, P.T., Sheel, M., et al. (2014). Type I IFN signaling in CD8- DCs impairs Th1-dependent malaria immunity. J. Clin. Invest. *124*, 2483–2496.

Hayden, M.S., and Ghosh, S. (2008). Shared principles in NF-kappaB signaling. Cell *132*, 344–362.

Langhorne, J., Ndungu, F.M., Sponaas, A.M., and Marsh, K. (2008). Immunity to malaria: more questions than answers. Nat. Immunol. *9*, 725–732.

Li, J., Pattaradilokrat, S., Zhu, F., Jiang, H., Liu, S., Hong, L., Fu, Y., Koo, L., Xu, W., Pan, W., et al. (2011). Linkage maps from multiple genetic crosses and loci linked to growth-related virulent phenotype in Plasmodium yoelii. Proc. Natl. Acad. Sci. USA *108*, E374–E382.

Liehl, P., and Mota, M.M. (2012). Innate recognition of malarial parasites by mammalian hosts. Int. J. Parasitol. *42*, 557–566.

Liehl, P., Zuzarte-Luís, V., Chan, J., Zillinger, T., Baptista, F., Carapau, D., Konert, M., Hanson, K.K., Carret, C., Lassnig, C., et al. (2014). Host-cell sensors for Plasmodium activate innate immunity against liver-stage infection. Nat. Med. *20*, 47–53.

Liu, Y.J. (2005). IPC: professional type 1 interferon-producing cells and plasmacytoid dendritic cell precursors. Annu. Rev. Immunol. *23*, 275–306.

Meredith, M.M., Liu, K., Darrasse-Jeze, G., Kamphorst, A.O., Schreiber, H.A., Guermonprez, P., Idoyaga, J., Cheong, C., Yao, K.H., Niec, R.E., and Nussenzweig, M.C. (2012). Expression of the zinc finger transcription factor zDC (Zbtb46, Btbd4) defines the classical dendritic cell lineage. J. Exp. Med. *209*, 1153–1165.

Miller, L.H., Ackerman, H.C., Su, X.Z., and Wellems, T.E. (2013). Malaria biology and disease pathogenesis: insights for new treatments. Nat. Med. *19*, 156–167.

Miller, J.L., Sack, B.K., Baldwin, M., Vaughan, A.M., and Kappe, S.H. (2014). Interferon-mediated innate immune responses against malaria parasite liver stages. Cell Rep. *7*, 436–447.

Nakagawa, R., Naka, T., Tsutsui, H., Fujimoto, M., Kimura, A., Abe, T., Seki, E., Sato, S., Takeuchi, O., Takeda, K., et al. (2002). SOCS-1 participates in negative regulation of LPS responses. Immunity *17*, 677–687.

O'Connell, R.M., Saha, S.K., Vaidya, S.A., Bruhn, K.W., Miranda, G.A., Zarnegar, B., Perry, A.K., Nguyen, B.O., Lane, T.F., Taniguchi, T., et al. (2004). Type I interferon production enhances susceptibility to Listeria monocytogenes infection. J. Exp. Med. *200*, 437–445.

Palomo, J., Fauconnier, M., Coquard, L., Gilles, M., Meme, S., Szeremeta, F., Fick, L., Franetich, J.F., Jacobs, M., Togbe, D., et al. (2013). Type I interferons contribute to experimental cerebral malaria development in response to sporozoite or blood-stage Plasmodium berghei ANKA. Eur. J. Immunol. *43*, 2683–2695.

Paludan, S.R., and Bowie, A.G. (2013). Immune sensing of DNA. Immunity *38*, 870–880.

Riley, E.M., and Stewart, V.A. (2013). Immune mechanisms in malaria: new insights in vaccine development. Nat. Med. *19*, 168–178.

Sharma, S., DeOliveira, R.B., Kalantari, P., Parroche, P., Goutagny, N., Jiang, Z., Chan, J., Bartholomeu, D.C., Lauw, F., Hall, J.P., et al. (2011). Innate immune recognition of an AT-rich stem-loop DNA motif in the Plasmodium falciparum genome. Immunity *35*, 194–207.

Sharma, S., Campbell, A.M., Chan, J., Schattgen, S.A., Orlowski, G.M., Nayar, R., Huyler, A.H., Nündel, K., Mohan, C., Berg, L.J., et al. (2015). Suppression of systemic autoimmunity by the innate immune adaptor STING. Proc. Natl. Acad. Sci. USA *112*, E710–E717.

Stevenson, M.M., and Riley, E.M. (2004). Innate immunity to malaria. Nat. Rev. Immunol. *4*, 169–180.

Sun, L., Wu, J., Du, F., Chen, X., and Chen, Z.J. (2013). Cyclic GMP-AMP synthase is a cytosolic DNA sensor that activates the type I interferon pathway. Science *339*, 786–791.

Swiecki, M., Gilfillan, S., Vermi, W., Wang, Y., and Colonna, M. (2010). Plasmacytoid dendritic cell ablation impacts early interferon responses and antiviral NK and CD8(+) T cell accrual. Immunity *33*, 955–966.

Takeuchi, O., and Akira, S. (2010). Pattern recognition receptors and inflammation. Cell *140*, 805–820.

Teijaro, J.R., Ng, C., Lee, A.M., Sullivan, B.M., Sheehan, K.C., Welch, M., Schreiber, R.D., de la Torre, J.C., and Oldstone, M.B. (2013). Persistent LCMV infection is controlled by blockade of type I interferon signaling. Science *340*, 207–211.

Teles, R.M., Graeber, T.G., Krutzik, S.R., Montoya, D., Schenk, M., Lee, D.J., Komisopoulou, E., Kelly-Scumpia, K., Chun, R., Iyer, S.S., et al. (2013). Type I interferon suppresses type II interferon-triggered human anti-mycobacterial responses. Science *339*, 1448–1453.

Togbe, D., Schofield, L., Grau, G.E., Schnyder, B., Boissay, V., Charron, S., Rose, S., Beutler, B., Quesniaux, V.F., and Ryffel, B. (2007). Murine cerebral malaria development is independent of toll-like receptor signaling. Am. J. Pathol. *170*, 1640–1648.

Voisine, C., Mastelic, B., Sponaas, A.M., and Langhorne, J. (2010). Classical CD11c+ dendritic cells, not plasmacytoid dendritic cells, induce T cell responses to Plasmodium chabaudi malaria. Int. J. Parasitol. *40*, 711–719.

Wang, Y., Swiecki, M., McCartney, S.A., and Colonna, M. (2011). dsRNA sensors and plasmacytoid dendritic cells in host defense and autoimmunity. Immunol. Rev. *243*, 74–90.

Wilson, E.B., Yamada, D.H., Elsaesser, H., Herskovitz, J., Deng, J., Cheng, G., Aronow, B.J., Karp, C.L., and Brooks, D.G. (2013). Blockade of chronic type I interferon signaling to control persistent LCMV infection. Science *340*, 202–207.

Wu, X., Gowda, N.M., Kumar, S., and Gowda, D.C. (2010). Protein-DNA complex is the exclusive malaria parasite component that activates dendritic cells and triggers innate immune responses. J. Immunol. *184*, 4338–4348.

Wu, J., Tian, L., Yu, X., Pattaradilokrat, S., Li, J., Wang, M., Yu, W., Qi, Y., Zeituni, A.E., Nair, S.C., et al. (2014). Strain-specific innate immune signaling pathways determine malaria parasitemia dynamics and host mortality. Proc. Natl. Acad. Sci. USA *111*, E511–E520.

Immunity, Volume *45*

Supplemental Information

Cross-Regulation of Two Type I Interferon Signaling Pathways in Plasmacytoid Dendritic Cells Controls Anti-malaria Immunity and Host Mortality

Xiao Yu, Baowei Cai, Mingjun Wang, Peng Tan, Xilai Ding, Jian Wu, Jian Li, Qingtian Li, Pinghua Liu, Changsheng Xing, Helen Y. Wang, Xin-zhuan Su, and Rong-Fu Wang

Supplemental online information

Cross-regulation of two type I interferon signaling pathways in plasmacytoid dendritic cells controls anti-malaria immunity and host mortality

Xiao Yu, Baowei Cai, Mingjun Wang, Peng Tan, Xilai Ding, Jian Wu, Jian Li, Qingtian Li, Pinghua Liu, Changsheng Xing, Helen Y. Wang, Xin-zhuan Su, and Rong-Fu Wang

Supplemental Figures: Figure S1-S7.

Supplemental Experiment Procedures

Figure S1

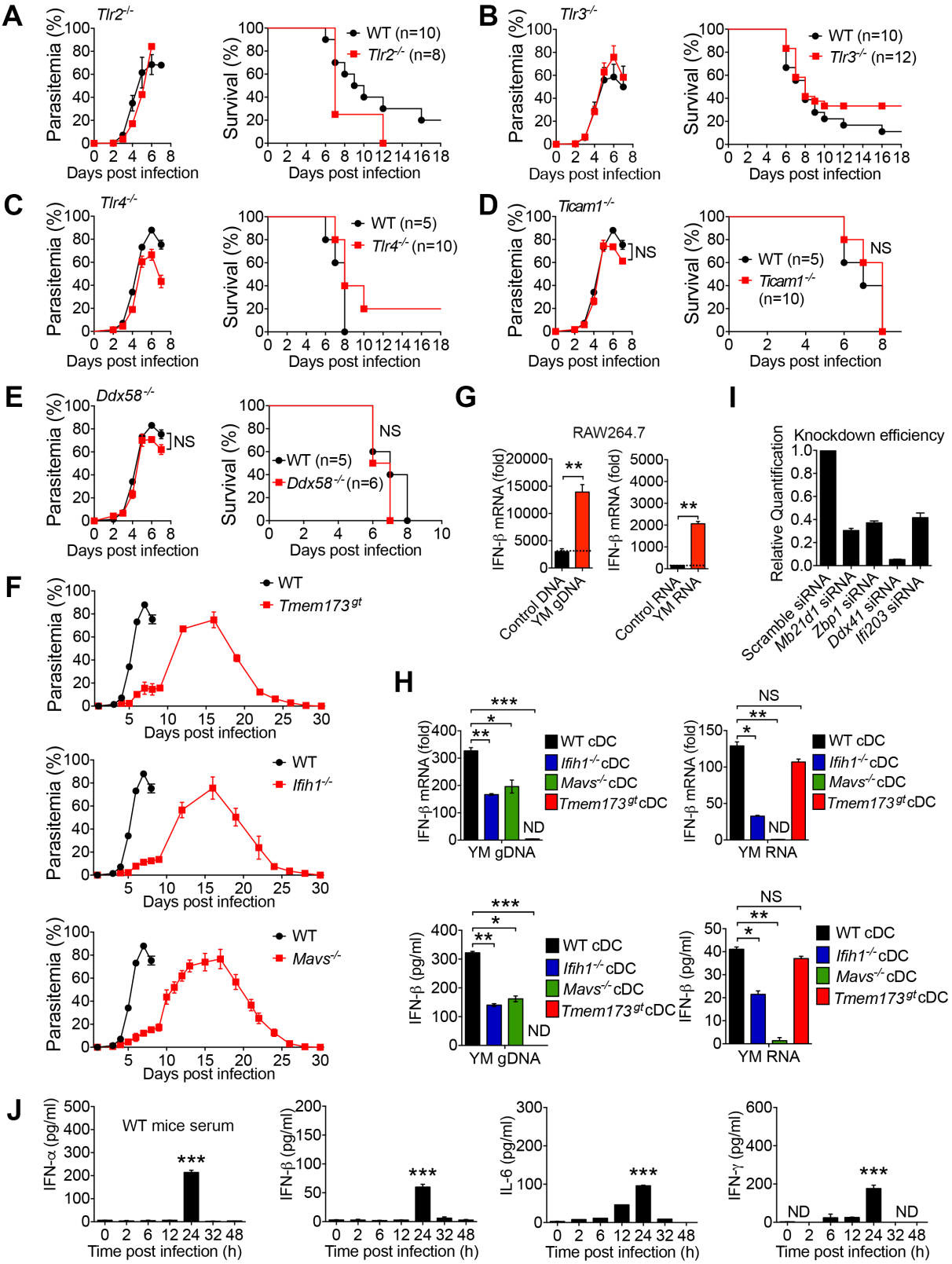
A
Tlr2-/-
Parasitemia (%)
Days post infection
Survival (%)
WT (n=10)
Tlr2-/- (n=8)
B
Tlr3-/-
WT (n=10)
Tlr3-/- (n=12)
C
Tlr4-/-
WT (n=5)
Tlr4-/- (n=10)
D
Ticam1-/-
NS
WT (n=5)
Ticam1-/- (n=10)
E
Ddx58-/-
WT (n=5)
Ddx58-/- (n=6)
F
WT
Tmem173gt
Ifih1-/-
Mavs-/-
G
RAW264.7
IFN-β mRNA (fold)
Control DNA
YM gDNA
Control RNA
YM RNA
I
Knockdown efficiency
Relative Quantification
Scramble siRNA
Mb21d1 siRNA
Zbp1 siRNA
Ddx41 siRNA
Ifi203 siRNA
H
WT cDC
Ifih1-/- cDC
Mavs-/- cDC
Tmem173gt cDC
ND
YM gDNA
YM RNA
IFN-β (pg/ml)
J
WT mice serum
IFN-α (pg/ml)
IFN-β (pg/ml)
IL-6 (pg/ml)
IFN-γ (pg/ml)
Time post infection (h)

Figure S1. *Tlr2*$^{-/-}$, *Tlr3*$^{-/-}$, *Tlr4*$^{-/-}$, *Ticam1*$^{-/-}$, and *Ddx58*$^{-/-}$ mice are susceptible to *Plasmodium yoelii* YM infection and Type I IFN gene expression after *P. yoelii* YM gDNA or RNA stimulation or serum cytokine production after *P. yoelii* YM infection. Related to Figure 1

(A-E) Daily YM parasitemias and mortality rates of WT (black lines) and deficient mice (red lines). C57BL/6 (WT), *Tlr2*$^{-/-}$, *Tlr3*$^{-/-}$, *Tlr4*$^{-/-}$, *Ticam1*$^{-/-}$, and *Ddx58*$^{-/-}$ mice were intraperitoneally infected with *P. yoelii* YM (0.2-0.5×10^6 iRBCs). *Tlr2*$^{-/-}$ **(A)**, *Tlr3*$^{-/-}$ **(B)**, *Tlr4*$^{-/-}$ **(C)**, *Ticam1*$^{-/-}$ **(D)**, and *Ddx58*$^{-/-}$ **(E)**. **(F)** Daily YM parasitemias of WT (black lines), *Ifih1*$^{-/-}$, *Mavs*$^{-/-}$, and *Tmem173*^{gt} mice (red lines) after *P. yoelii* YM (1×10^6 iRBCs). **(G)** Quantitative analysis of IFN-β mRNA in RAW264.7 cells stimulated with purified *P. yoelii* YM genomic DNA (gDNA) or RNA from YM-infected RBCs. gDNA or RNA purified from uninfected RBCs served as a control. **(H)** Quantitative analysis and ELISA analysis of IFN-β mRNA and protein amount in cDCs derived from WT and deficient (*Ifih1*$^{-/-}$, *Mavs*$^{-/-}$, and *Tmem173*^{gt}) mice after *P. yoelii* YM gDNA or RNA stimulation. **(I)** Silencing efficiency of *Mb21d1*, *Zbp1*, *Ddx41*, and *Ifi203* in RAW264.7 cells transfected with specific siRNAs for *Mb21d1*, *Zbp1*, *Ddx41*, *Ifi203* or scrambled siRNAs for 48 h. **(J)** Serum amounts of IFN-α, IFN-β, IL-6 and IFN-γ from WT mice at the indicated times after *P. yoelii* YM infection, assessed by ELISA. Data are plotted as the mean ± s.d. and are representative of three independent experiments. **P* <0.05, ***P* <0.01, ****P* <0.001 vs. corresponding control. ND, not detected; NS, not significant.

Figure S2

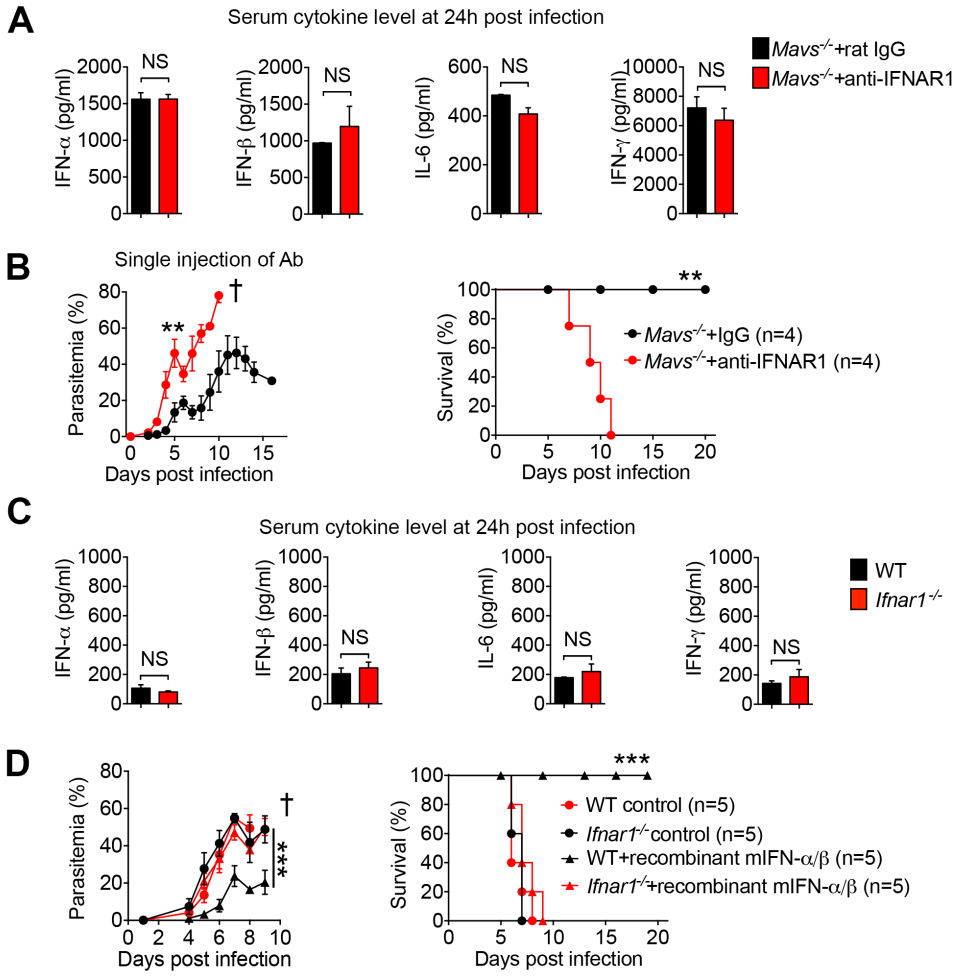

Figure S2. Blockage of type I IFN receptor determines the fate of *P. yoelii* YM infected mice. Related to Figure 2

(A) Serum amounts of IFN-α, IFN-β, IL-6, and IFN-γ collected at 24h after *P. yoelii* YM infection in *Mavs*$^{-/-}$ mice untreated or treated with anti-IFNAR1 blocking antibody (500 μg) single injection at 12 h before *P. yoelii* YM infection. **(B)** Parasitemias and mortality rates of *Mavs* $^{-/-}$ mice treated with anti-IFNAR1 blocking antibody (500 μg, single injection at 12h before infection), followed by infection with *P. yoelii* YM (2×10^6 iRBCs). **(C)** Serum amounts of IFN-α, IFN-β, IL-6, and IFN-γ in WT and *Ifnar1*$^{-/-}$ mice at 24 h after *P. yoelii* YM infection. **(D)** Parasitemias and mortality rates of WT and *Ifnar1*$^{-/-}$ mice infected with *P. yoelii* YM, followed by intravenous administration of recombinant mouse IFN-α and IFN-β at 18h post infection. Data are plotted as the mean ± s.d. and representative of three independent experiments. $^{**}P$ <0.01, $^{***}P$ <0.001 vs. corresponding control. NS, not significant. † denotes mouse death.

Figure S3

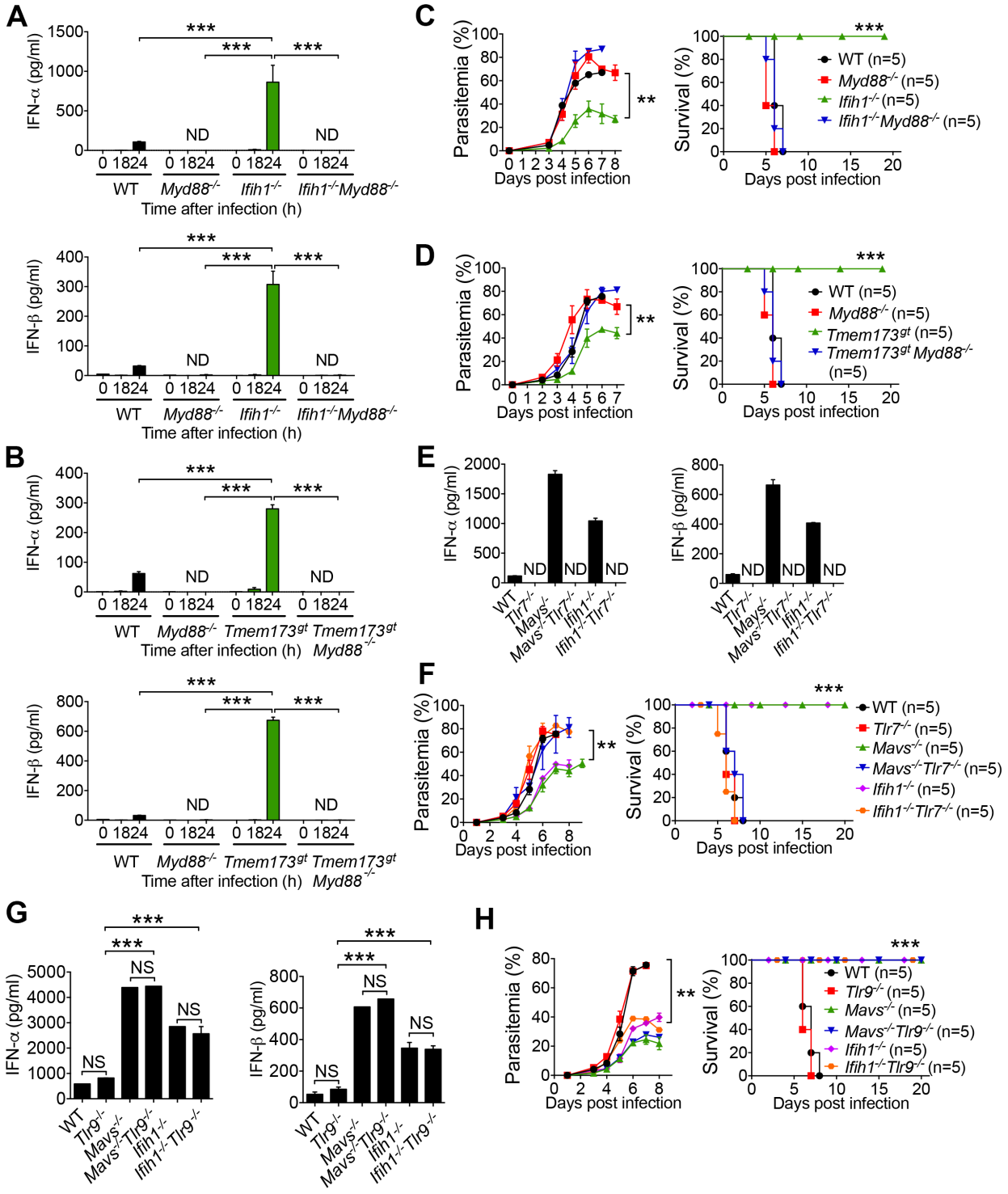
A
IFN-α (pg/ml)
IFN-β (pg/ml)
ND
WT
Myd88-/-
Ifih1-/-
Ifih1-/-Myd88-/-
Time after infection (h)
B
Tmem173gt
Myd88-/- Tmem173gt
C
Parasitemia (%)
Days post infection
Survival (%)
WT (n=5)
Myd88-/- (n=5)
Ifih1-/- (n=5)
Ifih1-/-Myd88-/- (n=5)
D
Tmem173gt (n=5)
Tmem173gt Myd88-/- (n=5)
E
Tlr7-/-
Mavs-/-
Mavs-/-Tlr7-/-
Ifih1-/-Tlr7-/-
F
Tlr7-/- (n=5)
Mavs-/- (n=5)
Mavs-/-Tlr7-/- (n=5)
Ifih1-/- (n=5)
Ifih1-/-Tlr7-/- (n=5)
G
Tlr9-/-
Mavs-/-Tlr9-/-
Ifih1-/-Tlr9-/-
NS
H
Tlr9-/- (n=5)
Mavs-/- (n=5)
Mavs-/-Tlr9-/- (n=5)
Ifih1-/- (n=5)
Ifih1-/-Tlr9-/- (n=5)

Figure S3. Requirement and regulation of TLR7-MyD88-IRF7 in type I IFN mediated protection of mice from *P. yoelii* YM infection. Related to Figure 3

(A-B) Serum amounts of IFN-α and IFN-β in WT and deficient (*Myd88*$^{-/-}$, *Ifih1*$^{-/-}$, *Ifih1*$^{-/-}$:*Myd88*$^{-/-}$, *Tmem173*^{gt} and *Tmem173*^{gt}:*Myd88*$^{-/-}$) mice at 0, 18, and 24 h after *P. yoelii* YM infection. **(C-D)** Daily YM parasitemias and mortality rates of WT and deficient (*Myd88*$^{-/-}$, *Ifih1*$^{-/-}$, *Ifih1*$^{-/-}$:*Myd88*$^{-/-}$, *Tmem173*^{gt} and *Tmem173*^{gt}:*Myd88*$^{-/-}$) mice after *P. yoelii* YM (1×10^6 iRBCs) infection. **(E)** Serum amounts of IFN-α and IFN-β in WT and deficient (*Tlr7*$^{-/-}$, *Mavs*$^{-/-}$, *Mavs*$^{-/-}$:*Tlr7*$^{-/-}$, *Ifih1*$^{-/-}$ and *Ifih1*$^{-/-}$:*Tlr7*$^{-/-}$) mice at 24 h after *P. yoelii* YM infection. **(F)** Daily YM parasitemias and mortality rates of WT and deficient (*Tlr7*$^{-/-}$, *Mavs*$^{-/-}$, *Mavs*$^{-/-}$:*Tlr7*$^{-/-}$, *Ifih1*$^{-/-}$ and *Ifih1*$^{-/-}$:*Tlr7*$^{-/-}$) mice after *P. yoelii* YM (1×10^6 iRBCs) infection. **(G)** Serum amounts of IFN-α and IFN-β in WT, *Tlr9*$^{-/-}$, *Mavs*$^{-/-}$, *Mavs*$^{-/-}$:*Tlr9*$^{-/-}$, *Ifih1*$^{-/-}$ and *Ifih1*$^{-/-}$:*Tlr9*$^{-/-}$ mice at 24 h after *P. yoelii* YM infection. **(H)** Daily YM parasitemias and mortality rates of WT and deficient (*Tlr9*$^{-/-}$, *Mavs*$^{-/-}$, *Mavs*$^{-/-}$:*Tlr9*$^{-/-}$, *Ifih1*$^{-/-}$ and *Ifih1*$^{-/-}$:*Tlr9*$^{-/-}$ mice) mice after *P. yoelii* YM (1×10^6 iRBCs) infection. Data are plotted as the mean ± s.d. and are representative of three independent experiments. $^{**}P<0.01$, $^{***}P<0.001$ vs. corresponding control. ND, not detected. NS, not significant.

Figure S4

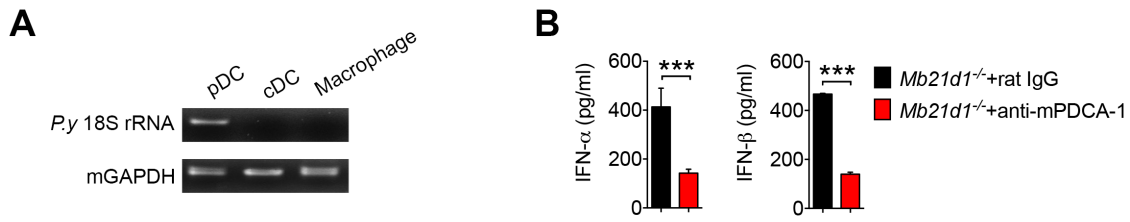

Figure S4. Detection of malaria 18S rRNA in pDCs, cDCs and macrophages and serum amount of type I IFN in cGAS-deficient mice after pDC depletion. Related to Figure 4

(A) The cell populations of pDCs, cDCs and macrophages were isolated from WT mice splenocytes at 18h post YM infection by cell isolation kits, and then analyzed for cell-specific expression of *P. yoelii* 18S rRNA by PCR. **(B)** Depletion of pDCs cell population in *Mb21d1*$^{-/-}$ mice by administration of anti-mPDCA-1 antibody at 12 h before and 12 h after YM infection, rat IgG treatment served as a control. Serum amounts of IFN-α and IFN-β collected at 24 h after infection in *Mb21d1*$^{-/-}$ mice untreated or treated with anti-mPDCA-1 are shown. Data are plotted as the mean ± s.d. and are representative of three independent experiments. ***P <0.001 vs. corresponding control.

Figure S5

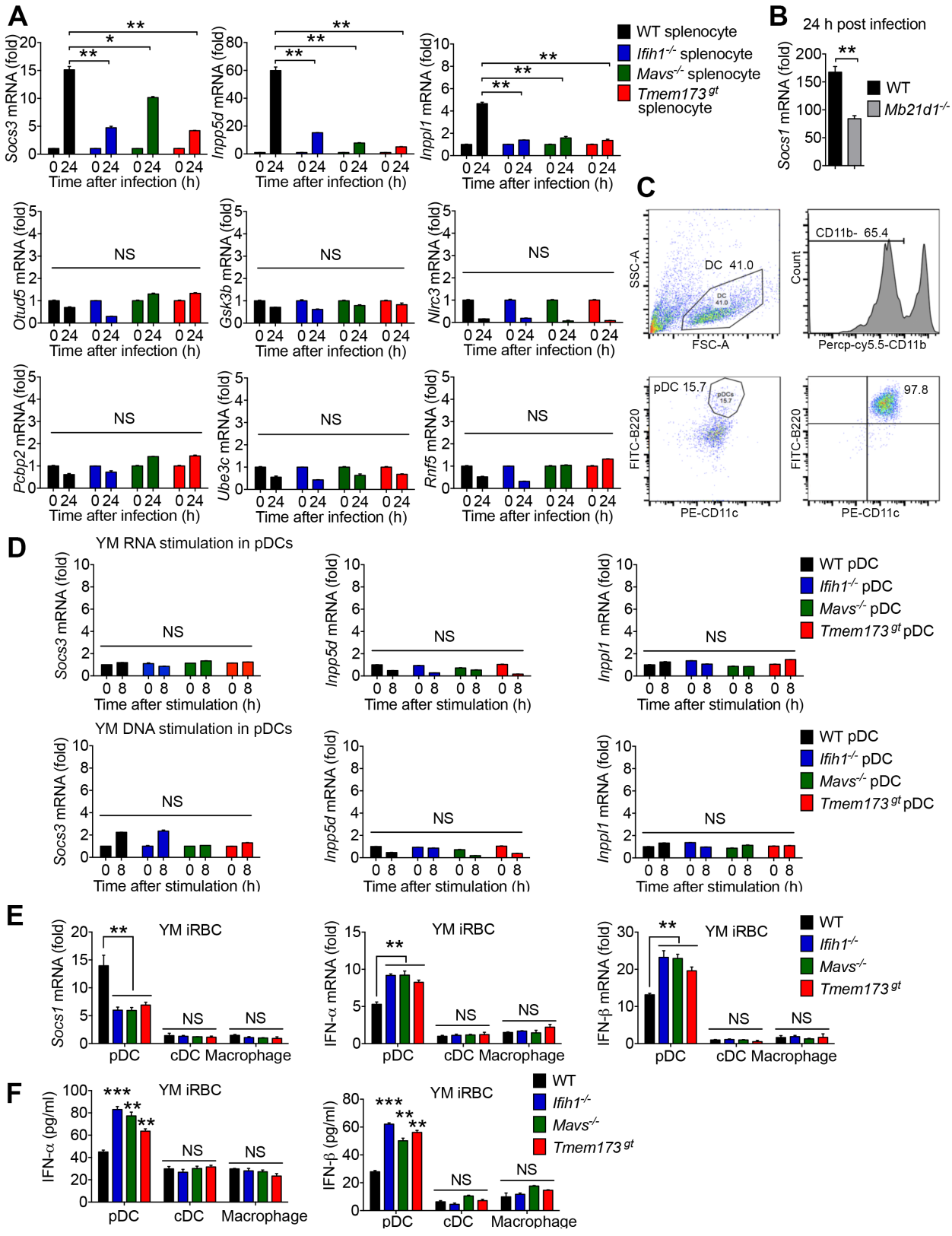
A
Socs3 mRNA (fold)
Inpp5d mRNA (fold)
Inppl1 mRNA (fold)
Time after infection (h)
WT splenocyte
Ifih1-/- splenocyte
Mavs-/- splenocyte
Tmem173gt splenocyte
Otud5 mRNA (fold)
Gsk3b mRNA (fold)
Nlrc3 mRNA (fold)
Pcbp2 mRNA (fold)
Ube3c mRNA (fold)
Rnf5 mRNA (fold)
NS
B
24 h post infection
Socs1 mRNA (fold)
WT
Mb21d1-/-
C
SSC-A
FSC-A
DC 41.0
Count
CD11b- 65.4
Percp-cy5.5-CD11b
pDC 15.7
FITC-B220
PE-CD11c
97.8
D
YM RNA stimulation in pDCs
YM DNA stimulation in pDCs
Time after stimulation (h)
WT pDC
Ifih1-/- pDC
Mavs-/- pDC
Tmem173gt pDC
E
YM iRBC
Socs1 mRNA (fold)
IFN-α mRNA (fold)
IFN-β mRNA (fold)
pDC
cDC
Macrophage
WT
Ifih1-/-
Mavs-/-
Tmem173gt
F
IFN-α (pg/ml)
IFN-β (pg/ml)

Figure S5. Identify putative negative regulators of type I interferon signaling after *P. yoelii* YM infection. Related to Figure 5

(A) Expression of putative negative regulators *Socs3*, *Inpp5d*, *Inppl1*, *Otud5*, *Gsk3b*, *Nlrc3*, *Pcbp2*, *Ube3c,* and *Rnf5* in the spleens of WT and deficient (*Ifih1*$^{-/-}$, *Mavs*$^{-/-}$, and *Tmem173*^{gt}) mice at the indicated times after *P. yoelii* YM infection. RNA from splenocytes was isolated and used for expression analysis using qPCR. **(B)** Expression of *Socs1* in the spleens of WT and *Mb21d1*$^{-/-}$ mice at 24 h after *P. yoelii* YM infection. RNA from splenocytes was isolated and used for expression analysis using qPCR. **(C)** Purification of pDCs (CD11b^{-}B220^{+}CD11c^{+}) by flow cytometry analysis. The last panel shows the percentage of pDCs after sorting. **(D)** Expression of *Socs3*, *Inpp5d* and *Inppl1* in pDCs of WT and deficient (*Ifih1*$^{-/-}$, *Mavs*$^{-/-}$, and *Tmem173*^{gt}) mice after *P. yoelii* YM RNA or gDNA stimulation. **(E)** Quantitative analysis of *Socs1* mRNA, IFN-α and IFN-β mRNA in pDCs, cDCs, and macrophages from WT and deficient (*Ifih1*$^{-/-}$, *Mavs*$^{-/-}$, and *Tmem173*^{gt}) mice after co-culture with *P. yoelii* YM iRBCs for 9 h. **(F)** ELISA analysis of IFN-α and IFN-β protein in supernatants of pDCs, cDCs, and macrophages from WT and deficient (*Ifih1*$^{-/-}$, *Mavs*$^{-/-}$, and *Tmem173*^{gt}) mice after co-culture with *P. yoelii* YM iRBCs for 24 h. Data are plotted as the mean ± s.d. and are representative of three independent experiments. **P* <0.05, ***P* <0.01, ****P* <0.001 vs. corresponding control. NS, not significant.

Figure S6

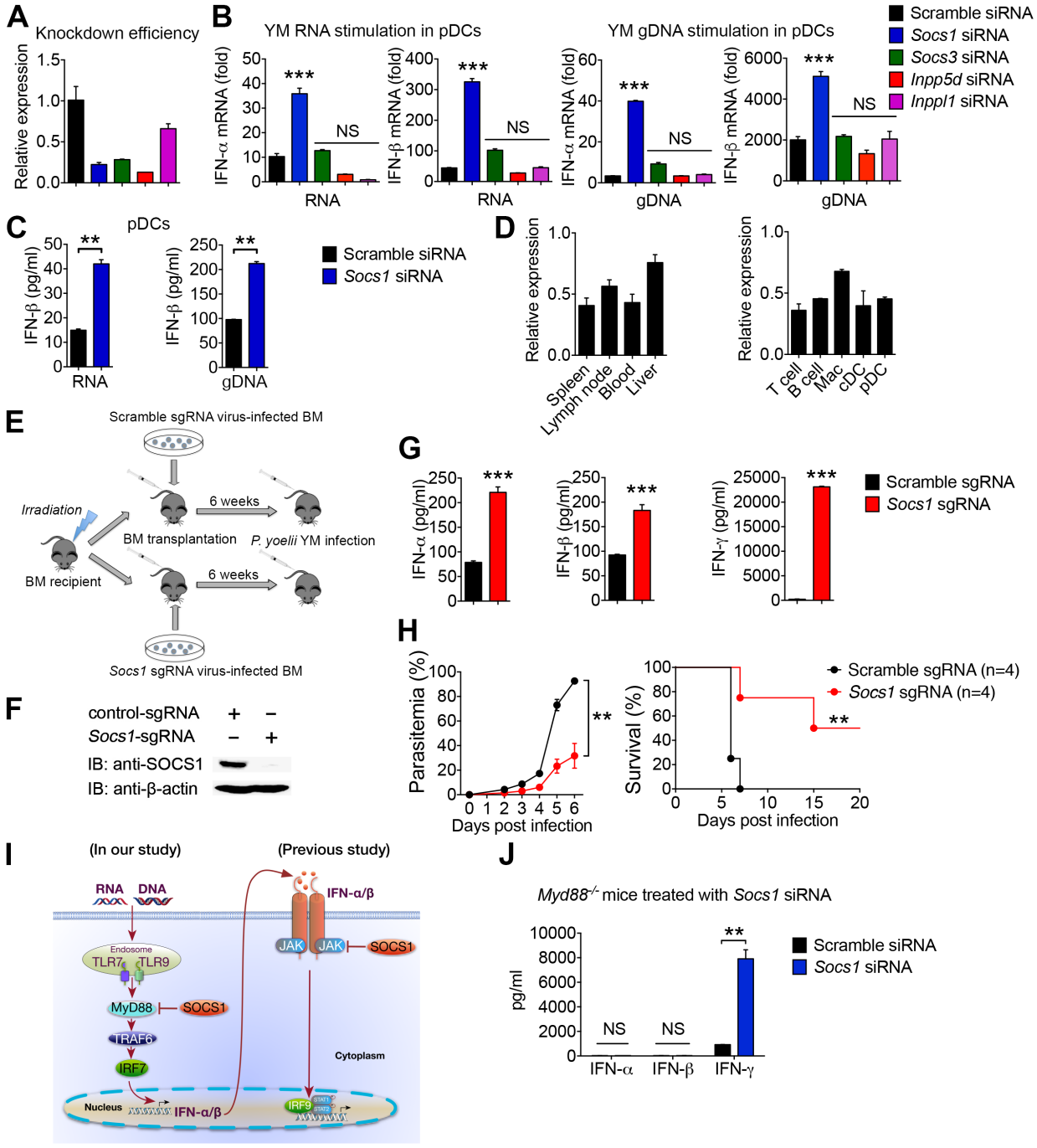
A
Knockdown efficiency
Relative expression
B
YM RNA stimulation in pDCs
YM gDNA stimulation in pDCs
IFN-α mRNA (fold)
IFN-β mRNA (fold)
RNA
gDNA
***
NS
Scramble siRNA
Socs1 siRNA
Socs3 siRNA
Inpp5d siRNA
Inppl1 siRNA
C
pDCs
IFN-β (pg/ml)
RNA
gDNA
**
Scramble siRNA
Socs1 siRNA
D
Relative expression
Spleen
Lymph node
Blood
Liver
T cell
B cell
Mac
cDC
pDC
E
Scramble sgRNA virus-infected BM
Irradiation
6 weeks
BM transplantation
P. yoelii YM infection
BM recipient
6 weeks
Socs1 sgRNA virus-infected BM
F
control-sgRNA + −
Socs1-sgRNA − +
IB: anti-SOCS1
IB: anti-β-actin
G
IFN-α (pg/ml)
IFN-β (pg/ml)
IFN-γ (pg/ml)
***
Scramble sgRNA
Socs1 sgRNA
H
Parasitemia (%)
Days post infection
Survival (%)
Days post infection
**
Scramble sgRNA (n=4)
Socs1 sgRNA (n=4)
I
(In our study)
(Previous study)
RNA
DNA
Endosome
TLR7
TLR9
MyD88
SOCS1
TRAF6
IRF7
Nucleus
IFN-α/β
IFN-α/β
JAK
JAK
SOCS1
Cytoplasm
IRF5
J
Myd88-/- mice treated with Socs1 siRNA
pg/ml
NS
NS
**
IFN-α
IFN-β
IFN-γ
Scramble siRNA
Socs1 siRNA

Figure S6. SOCS1 is responsible for inhibition of Myd88-dependent type I IFN in pDCs. Related to Figures 5 and 6

(A) Silencing efficiency of *Socs1*, *Socs3*, *Inpp5d* and *Inppl1* in pDCs transfected with specific siRNAs for *Socs1*, *Socs3*, *Inpp5d*, *Inppl1*, or scrambled siRNAs for 48 h. **(B)** Expression of IFN-α and IFN-β mRNA in WT pDCs transfected with *Socs1*-specific, *Socs3*-specific, *Inpp5d*-specific, *Inppl1*-specific, or scrambled siRNAs for 48h, followed by *P. yoelii* YM RNA or gDNA stimulation for 6 h. **(C)** IFN-β protein of pDCs transfected with *Socs1*-specific or scrambled siRNAs, followed by *P. yoelii* YM RNA or gDNA stimulation for 24 h. **(D)** Silencing efficiency of *Socs1* at 48 h after *Socs1*-specific siRNA delivery. C57BL/6 mice were injected intravenously with invivofectamine 3.0 (Invitrogen) mixed *Socs1*-specific siRNA or scrambled siRNA at dosage of 5mg/kg. Spleen, lymph node, liver and peripheral blood were collect at 48 h after siRNA injection and subjected to QPCR analysis of SOCS1 expression. Meanwhile, pDCs were isolated from spleen with anti-mPDCA-1 beads (Miltenyi); T cells, B cells, macrophages, and cDCs were isolated from spleen with PE-staining (CD3 for T cells, CD19 for B cells, F4/80 for macrophages and CD11c for cDCs, respectively.), followed by PE positive selection kit (Stemcell). RNA were isolated and subjected to QPCR analysis of SOCS1 expression. **(E)** Experimental procedure of genetically deletion of *Socs1* using CRISPR/CAS9 system in bone marrow for generating chimera mice. **(F)** Western blot analysis of *Socs1* deficiency in bone marrow cells after transduction with *Socs1*-specific or scrambled sgRNA lentiviral supernatant for 48 h. **(G)** Serum amounts of IFN-α, IFN-β, and IFN-γ in *Socs1*-specific or scramble sgRNA-treated mice at 24 h after *P. yoelii* YM infection. **(H)** Daily YM parasitemias and mortality rates of *Socs1*-specific or scrambled sgRNA-treated mice after *P. yoelii* YM infection. **(I)** A working model to explain SOCS1 inhibits Myd88 dependent type I IFN signaling and Jak1 dependent downstream signaling of type I IFN. (**J**) Serum amounts of IFN-α, IFN-β, and IFN-γ in *Socs1*-specific or scramble siRNA-treated *Myd88*$^{-/-}$ mice at 24 h after *P. yoelii* YM infection. Data are plotted as the mean ± s.d. and are representative of three independent experiments. $^{**}P < 0.01$, $^{***}P < 0.001$ vs. corresponding control. NS, not significant.

Figure S7

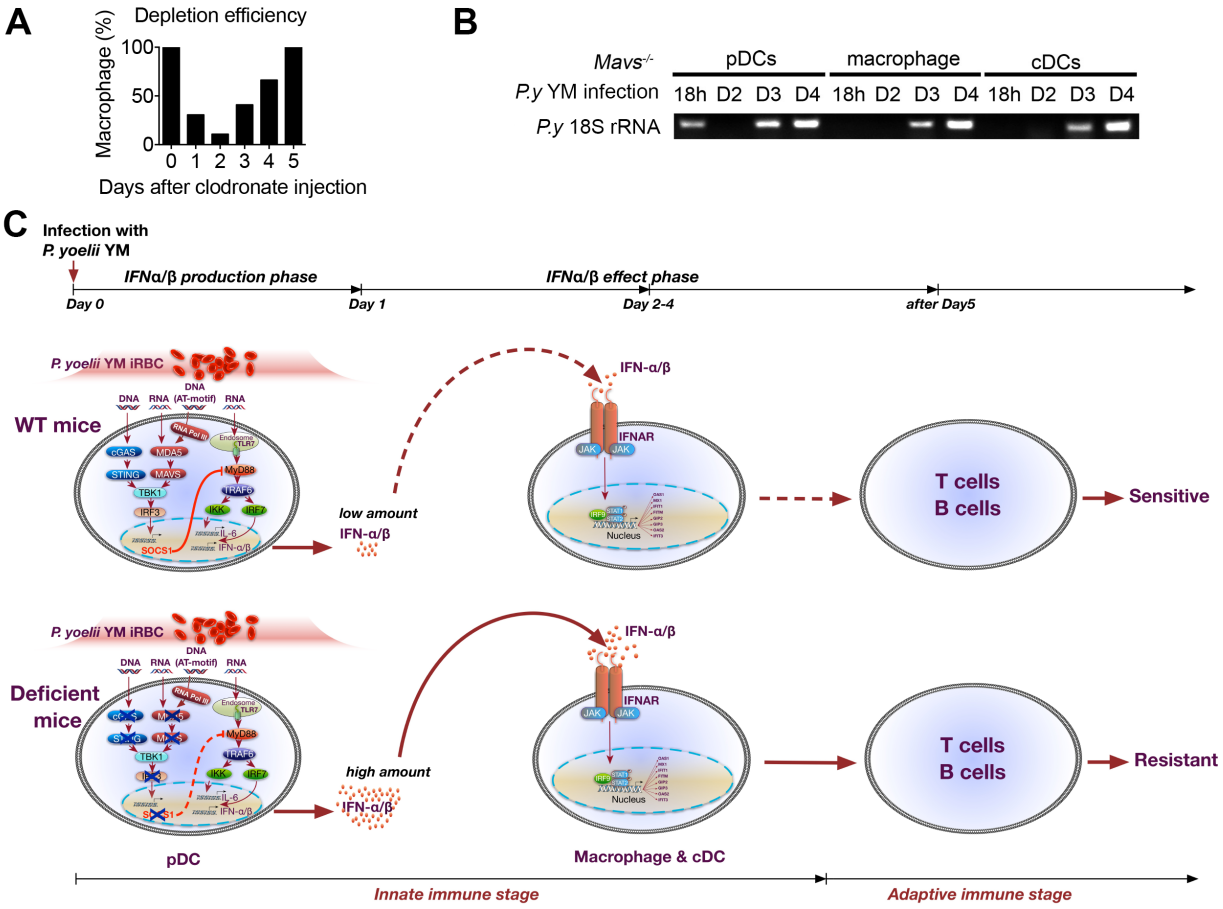

Figure S7. Stage-specific role of pDCs, cDCs, macrophages, T cells and B cells in generating IFN-α/β-induced immunity. Related to Figures 7

(A) *Tmem173*^{gt} mice were injected with clodronate (750 μg, intraperitoneally) and peripheral blood was collected at the indicated times and stained with CD11b, F4/80 for the flow cytometry analysis of macrophage percentage. Percentage of macrophage was compared to which in untreated mice. **(B)** The cell populations of pDC, cDC and macrophage were isolated from *Mavs*$^{-/-}$ mice splenocytes at indicated times post YM infection by cell isolation kits, and then analyzed for cell-specific expression of *P. yoelii* 18S rRNA by PCR. **(C)** A working model to illustrate how DNA/RNA sensors (cGAS, MDA5 and TLR7) detect malaria infection to activate two type I IFN signaling pathways in pDCs and the stage-specific roles of pDCs, macrophages, cDCs and T/B cells in generating IFN-α/β-induced immunity. Importantly, cGAS-STING and MDA5-MAVS-induced IRF3-dependent type I IFN signaling inhibits TLR7-MyD88-induced IRF7-dependent type IFN signaling pathway through upregulation of SOCS1 in WT pDCs in response to lethal *P. yoelii* YM infection. Deficiency in cGAS, STING, MDA5, MAVS or

IRF3 markedly increases IFN-α and IFN-β production at the early stage of infection (24 h) in deficient pDCs in response to lethal *P. yoelii* YM infection. Data are plotted as the mean ± s.d. and are representative of three independent experiments. ***P* <0.01, ****P* <0.001 vs. corresponding control. NS, not significant. † denotes mouse death.

Supplemental Experiment Procedures

Malaria parasites and mice

The parasite *Plasmodium yoelii* YM has been previously described (Li et al., 2011). For *plasmodium* infection, 1×10^6 iRBCs (otherwise, indicated specifically in the figure legend) suspended in 200 µl PBS from the donor mice were intraperitoneally injected into experimental mice. Parasitemias were monitored daily by examination of Giemsa-stained thin tail blood smears. Female mice of C57BL/6 (WT), *BDCA2-DTR*, *Zbtb46-DTR, Ifnar1*$^{-/-}$, *Mavs*$^{-/-}$, *Ifih1*$^{-/-}$, *Myd88*$^{-/-}$, *Tmem173*^{gt}, *Ticam1*$^{-/-}$, *Tlr2*$^{-/-}$, *Tlr3*$^{-/-}$, and *Tlr4*$^{-/-}$ mice were purchased from The Jackson Laboratory. *Tlr9*$^{-/-}$ mice were a gift from Dr. Marco Colonna (Washington University School of Medicine, St. Louis, MO), *Tlr7*$^{-/-}$ mice from Dr. Richard A. Flavell (Yale University, New Haven, CT), *Ddx58*$^{-/-}$ mice from Dr. Wenxin Wu (University of Oklahoma Health Science Center), *Irf3*$^{-/-}$:*Irf7*$^{-/-}$ mice from Dr. Kate Fitzgerald (University of Massachusetts Medical School) and Dr. Tadatsugo Taniguchi (The University of Tokyo), and *Mb21d1*$^{-/-}$ mice from Dr. Skip Virgin (Washington University at St. Luis). All mouse-related procedures were performed according to experimental protocols approved by the Animal Care and Welfare Committee at Houston Methodist Research Institute and in accordance with NIH–approved animal study protocol LMVR-11E.

***In vivo* receptor blockade, cytokine treatment, and cell depletion**

To block type I IFN receptor, anti-mouse interferon α/β receptor antibodies (Leinco Technologies), in the amount of 500 µg in PBS at day 0, 2, 4, and 250 µg at day 6 after infection (or indicated specifically in the figure legend), were intraperitoneally injected into WT and deficient mice. Mouse IgG antibody was used as control, and parasitemias were monitored by daily Giemsa-stained blood smears. To test the role of type I IFN cytokines, C57BL/6 mice were first infected with *P. yoelii* YM, and then intravenously injected with 800 U/g body weight mouse recombinant IFN-α and IFN-β, recombinant IL-6, or recombinant IFN-γ at the indicated time points. Bovine serum albumin (BSA, 0.1%) in PBS served as a control, and parasitemias were monitored by daily Giemsa-stained blood smears. To deplete pDCs, pDC-depleting functional-grade mAb (anti-mPDCA-1 IgG, clone JF05-1C2.4.1) was purchased from Miltenyi Biotec (Auburn, CA), and the corresponding isotype control IgG served as control. Two intraperitoneally injections of antibody (250 µg/mouse) per mouse were administered 12 h prior and after plasmodium YM infection or indicated specifically in the figure legend. To deplete macrophage, clodronate liposomes (from Dr. Nico. Van Rooijen) were injected intraperitoneally at 750 µg/injection at the indicated times, control liposomes served as control. T cells were depleted by intraperitoneally injection of anti-CD4 and anti-CD8 antibody every 3 days from 1 day before infection. B cells were depleted by intraperitoneally injection of anti-CD20 antibody every 4 days from 7 days before infection.

Isolation and preparation of *plasmodium* gDNA and RNA

Parasite-infected mice blood was collected in saline solution and filtered to deplete white blood cells. Parasites were spun down after RBC lysis buffer treatment, and lysate incubated with buffer A (150 mM NaCl, 25 mM EDTA, 10% SDS and protein kinase) overnight. gDNAs were isolated using phenol/chloroform, and RNAs were isolated using TRIzol reagent (Invitrogen).

Isolation and purification of immune cell populations

Bone marrow cells were isolated from the tibia and femur and cultured in RPMI1640 medium with 10% FBS, 1% penicillin-streptomycin, 55 µM β-mercaptoethanol, and 10% L929 conditioned media, containing macrophage-colony stimulating factor (M-CSF) for 5 days for BMDMs, 20 ng/ml murine GM-CSF and 10 ng/ml IL-4 for 6-8 days for cDCs. pDCs were generated from bone marrow in the culture medium containing 200 ng/ml Flt3L and further purified by flow cytometry analysis and were gated on the $CD11b^-B220^+CD11c^+$ cell population. For specific cell isolation from splenocytes, pDCs were isolated using anti-mPDCA-1 microbeads from Miltenyi Biotec (Auburn, CA). After pDC isolation, macrophages were isolated with CD11b microbeads from Miltenyi Biotec, cDCs were isolated with

mouse CD11cPE labeling and followed by PE selection cocktail from STEMCELL technologies, following the manufacturer's protocol.

Cell culture, transfection, immunoprecipitation and immunoblot analysis

HEK293T and RAW264.7 cells were maintained in DMEM (Hyclone) containing 10% FBS. STING stably expressing HEK293T cells (2×10^5) were plated in 24-well plates and transfected, through the use of Lipofectamine 2000 (Invitrogen), with 100 ng plasmids encoding Flag-tagged cGAS, DAI, DDX41, IFI16 or empty vector for 24 h, then stimulated with 1 ug YM gDNA or control DNA. Cells were collected at 18 h after DNA stimulation, and RNA were purified and subjected to QPCR analysis of IFN-β expression. For immunoprecipitation, 293T cells were transfected with 200 ng HA tagged SOCS1 and 300 ng Flag tagged IRAK1, IRAK4 or Myd88 for 48 h. Whole-cells extracts were prepared after transfection, followed by incubation overnight with the anti-Flag antibodies plus Protein A/G beads (Pierce). Beads were then washed five times with low-salt lysis buffer, and immunoprecipitates were eluted with 4×SDS loading buffer and resolved by SDS-PAGE. Proteins were transferred to nitrocellulose membranes (Bio-Rad) followed by further incubation with the appropriate antibodies. LumiGlo Chemiluminescent Substrate System was used for protein detection.

RNAi-mediated silencing in mice

In Vivo Ready siRNAs were mixed with Invivofectamine 3.0 liposomes (Invitrogen) following the manufacturer's instructions and injected intravenously in a volume of 100 µl at a dose of 5 mg/kg. Mice were infected with *P. yoelii* YM (0.5×10^6 iRBCs) at 48 h after siRNA treatment.

RNA preparation and qPCR

Total RNA was harvested from splenic tissue or stimulated cells using the TRIzol reagent (Invitrogen), and the complimentary cDNA was generated using reverse transcriptase III (Invitrogen). Real-time PCR was carried out using the ABI Prism 7000 analyzer (Applied Biosystems) using the SYBR GreenER qPCR Super Mix Universal (Invitrogen) and specific primers.

Isolation and purification of pDCs and Transfection with RNAi

Bone marrow cells were isolated and cultured with 200 ng/ml Flt3L for 9 days and isolated by flow cytometry analysis for pDCs ($CD11b^-B220^+CD11c^+$). siRNA oligonucleotides specific for *Mb21d1*, *Zbp1*, *Ddx41*, *Ifi203*, *Socs1*, *Socs3*, *Inpp5d*, *Inppl1*, and control (scrambled siRNA) were purchased from Invitrogen and nucleotransfected into RAW264.7 cells or pDCs cells for 48 h using Amaxa nucleofector kit, following the manufacturer's instructions (Lonza). Next, cells were stimulated with 1 µg *plasmodium* gDNA or RNA, using Lipofectamine 2000 reagent (Invitrogen), at the indicated time points. Supernatants were tested for cytokine production by ELISA, and RNAs were extracted for qPCR assay.

Mouse bone marrow transplant

Total bone marrow was isolated from the femurs and tibias from 8-week-old female C57BL/6 mice. Bone marrow was subjected to erythrocyte lysis, and then transduced with concentrated *Socs1*-specific or scrambled sgRNA lentiviral supernatant in the presence of 2 µg/ml polybrene. At 24 h post transduction, cells were collected and intravenously injected into lethally irradiated (950 cGy) 6-week-old female C57BL/6 mice.

Diphtheria Toxin (DT) treatment

Ifih1$^{-/-}$, *Mavs*$^{-/-}$ and *Tmem173*^{gt} mice were crossed with *BDCA2-DTR* transgenic mice to generate *Ifih1*$^{-/-}$:*BDCA2-DTR, Mavs*$^{-/-}$*:BDCA2-DTR* and *Tmem173*^{gt}*:BDCA2-DTR* mice, respectively, and then treated with diphtheria toxin (DT, Sigma-Aldrich) intraperitoneally (i.p.) at dose of 100-120 ng/mouse. pDCs were depleted by DT injection at 1 day before and 1, 3, and 5 days after *P. yoelii* YM infection. For cDC depletion, bone marrow chimeras were reconstituted for at least 6 to 8 weeks after lethal irradiation (950

cGy) and *i.v.* transferred with 10×10^6 bone marrow cells from *Mavs*$^{-/-}$:*Zbtb46-DTR* mice, then injected with DT at a dose of 2.5 ng per gram of body weight.

Statistical Analysis

All analyses were performed using GraphPad Prism version 5.0 (GraphPad Software, La Jolla, CA). Data are presented as means ± s.d., unless otherwise stated. Statistical significance of differences between two groups was assessed by unpaired Student *t* tests and a *p* value of <0.05 was considered significant.